Supplementary data for

Synthesis and singlet oxygen generation of pyrazinoporphyrazines containing dendrimeric aryl substituents

Adam Tillo[a], Dariusz T. Mlynarczyk[a], Lukasz Popenda[b], Barbara Wicher[a], Michal Kryjewski*[c], Wojciech Szczolko[a], Stefan Jurga[b,d], Jadwiga Mielcarek[c], Maria Gdaniec[e], Tomasz Goslinski[a], Ewa Tykarska*[a]

a. Department of Chemical Technology of Drugs, Poznan University of Medical Sciences, Grunwaldzka 6, 60-780 Poznan, Poland, E-mail: etykarsk@ump.edu.pl

b. NanoBioMedical Centre, Adam Mickiewicz University, Umultowska 85, 61-614 Poznan, Poland

c. Department of Inorganic and Analytical Chemistry, Poznan University of Medical Sciences, Grunwaldzka 6, 60-780 Poznan, Poland, E-mail: mkryjewski@ump.edu.pl

d. Department of Macromolecular Physics, Faculty of Physics, Adam Mickiewicz University, Umultowska 85, 61-614 Poznan, Poland

e. Faculty of Chemistry, Adam Mickiewicz University, Umultowska 89b, 61-614 Poznan, Poland

*Corresponding authors. Tel. +48 61 854 6632; fax. +48 61 854 6639; e-mail address: etykarsk@ump.edu.pl, (E. Tykarska); Tel. +48 61 854 6606; fax. +48 61 854 6609; e-mail address: mkryjewski@ump.edu.pl (M. Kryjewski)

Table of Contents

NMR data of **5b**

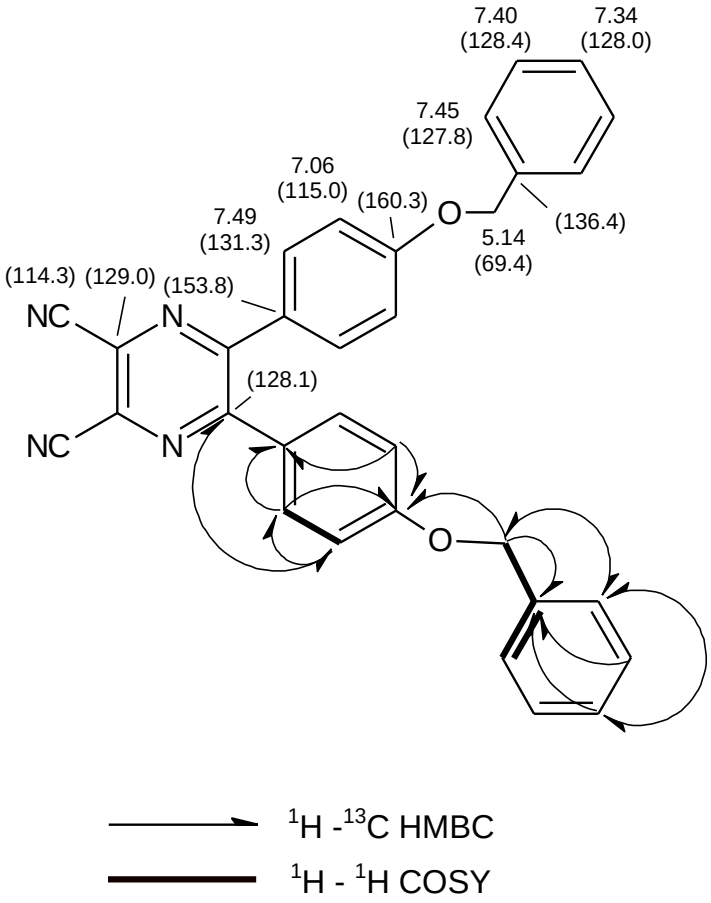

Fig. S1. ^{1}H and (^{13}C) chemical shift values [ppm] of **5b**. Key ^{1}H-^{13}C HMBC and ^{1}H-^{1}H COSY correlations are marked with arrows and bold lines, respectively.

Table S1. ^{1}H and ^{13}C NMR data obtained for **5b** including key correlations determined from ^{1}H-^{13}C HSQC and ^{1}H-^{13}C HMBC spectra.

δ_H (ppm)	**Multiplicity (J_{H-H} in Hz)**	**^{1}H-^{13}C HSQC δ_C (ppm)**	**^{1}H-^{13}C HMBC δ_C (ppm)**			
7.49	d (7.5)	131.3	115.0	153.8	160.3	
7.45	d (7.5)	127.8	69.4	128.0		
7.40	t(7.5)	128.4	136.4			
7.34	t (7.5)	128.0	127.8	136.4		
7.06	d (7.0)	115.0	128.1	131.3	153.8	160.3
5.14	s	69.4	127.8	136.4	160.3	
Quaternary carbon atoms (ppm): 114.3, 128.1, 129.0, 136.4, 153.8, 160.3						

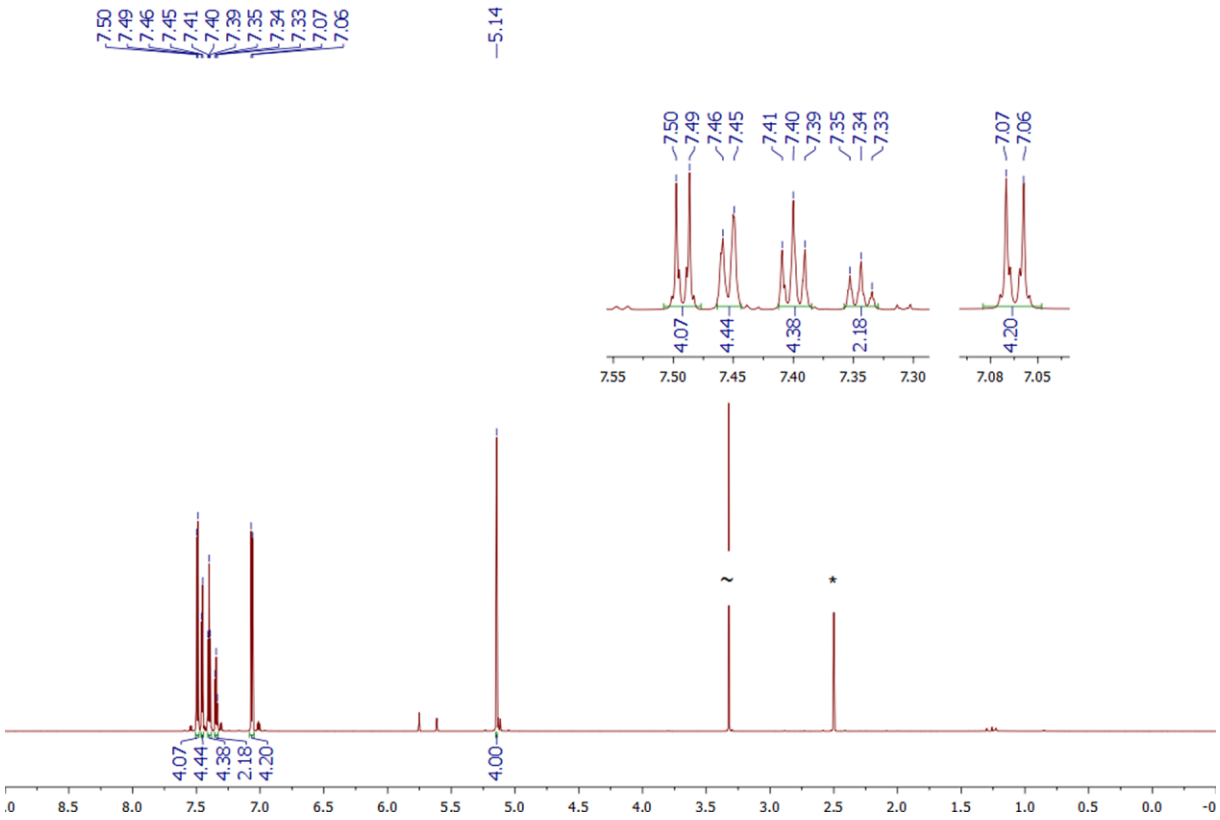

Fig. S2. [1]H NMR spectrum of **5b** (800 MHz, DMSO-d_6, 298 K). The symbols * and ~ indicate DMSO-d_6 and water residual peaks, respectively.

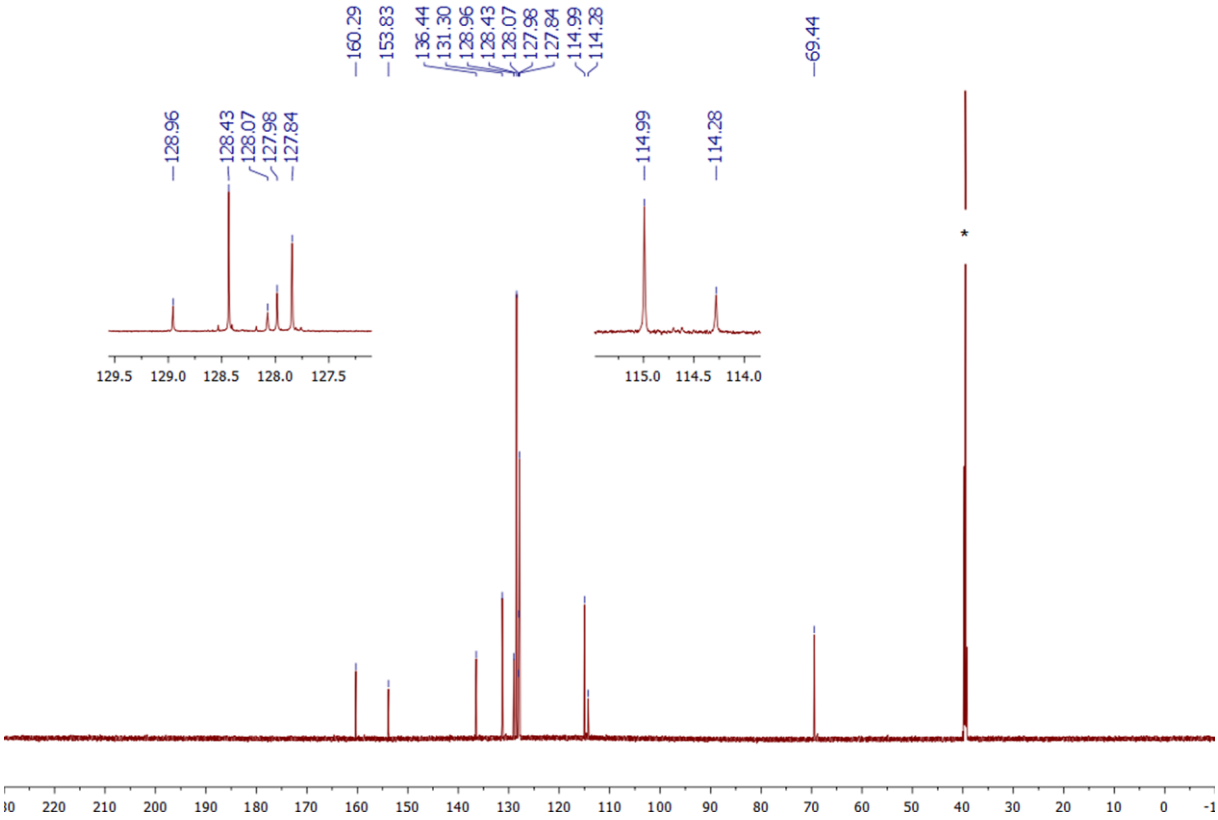

Fig. S3. [13]C NMR spectrum recorded for **5b** (201 MHz, DMSO-d_6, 298 K). The symbol * indicates DMSO-d_6 peak.

NMR data of **5c**

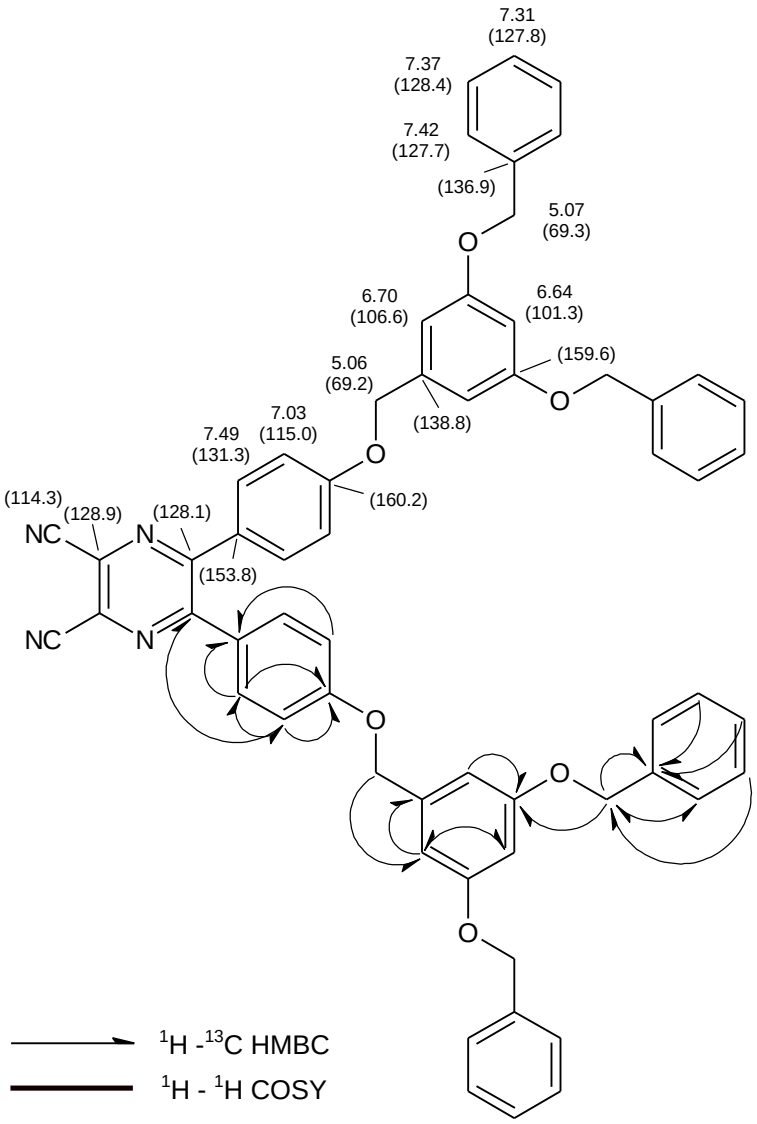

Fig. S4. ^{1}H and (^{13}C) chemical shift values [ppm] of **5c**. Key ^{1}H-^{13}C HMBC and ^{1}H-^{1}H COSY correlations are marked with arrows and bold lines, respectively.

Table. S2. ^{1}H and ^{13}C NMR data obtained for **5c** including key correlations determined from ^{1}H-^{13}C HSQC and ^{1}H-^{13}C HMBC spectra.

δ_H (ppm)	**Multiplicity (J_{H-H} in Hz)**	**^{1}H-^{13}C HSQC δ_C (ppm)**	**^{1}H-^{13}C HMBC δ_C (ppm)**
7.49	d (7.5)	131.3	115.0 153.8 160.2
7.42	d (7.5)	127.7	69.3
7.37	t (7.5)	128.4	69.3 136.9
7.31	m	127.8	136.9
7.03	d (7.0)	115.0	128.1 131.3 153.8 160.2
6.70	d (2.4)	106.6	101.3 138.8 159.6
6.64	t (2.4)	101.3	106.6
5.07	s	69.3	127.7 136.9 159.6
5.06	s	69.2	106.6
Quaternary carbon atoms (ppm): 114.3, 128.1, 128.9, 136.9, 138.8, 153.8, 159.6, 160.2			

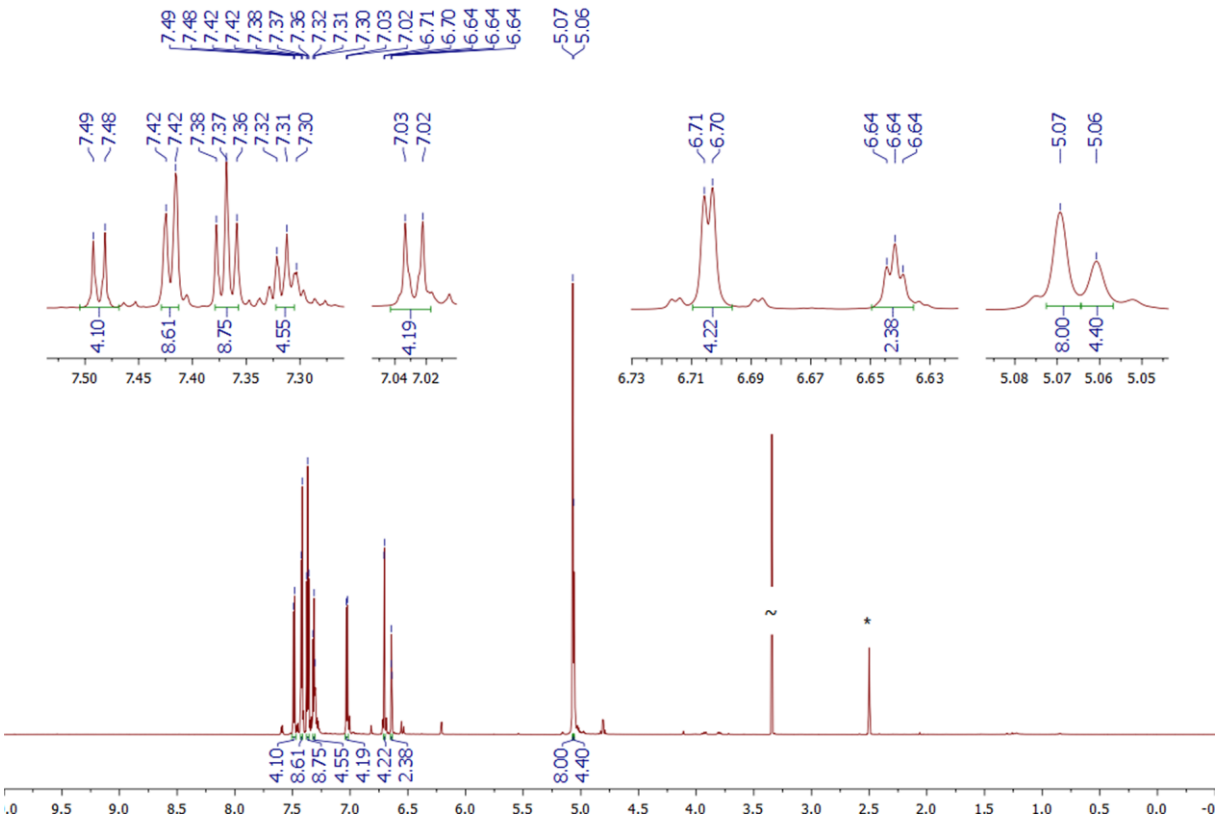

Fig. S5. [1]H NMR spectrum of **5c** (800 MHz, DMSO-d_6, 298 K). The symbols * and ~ indicate DMSO-d_6 and water residual peaks, respectively.

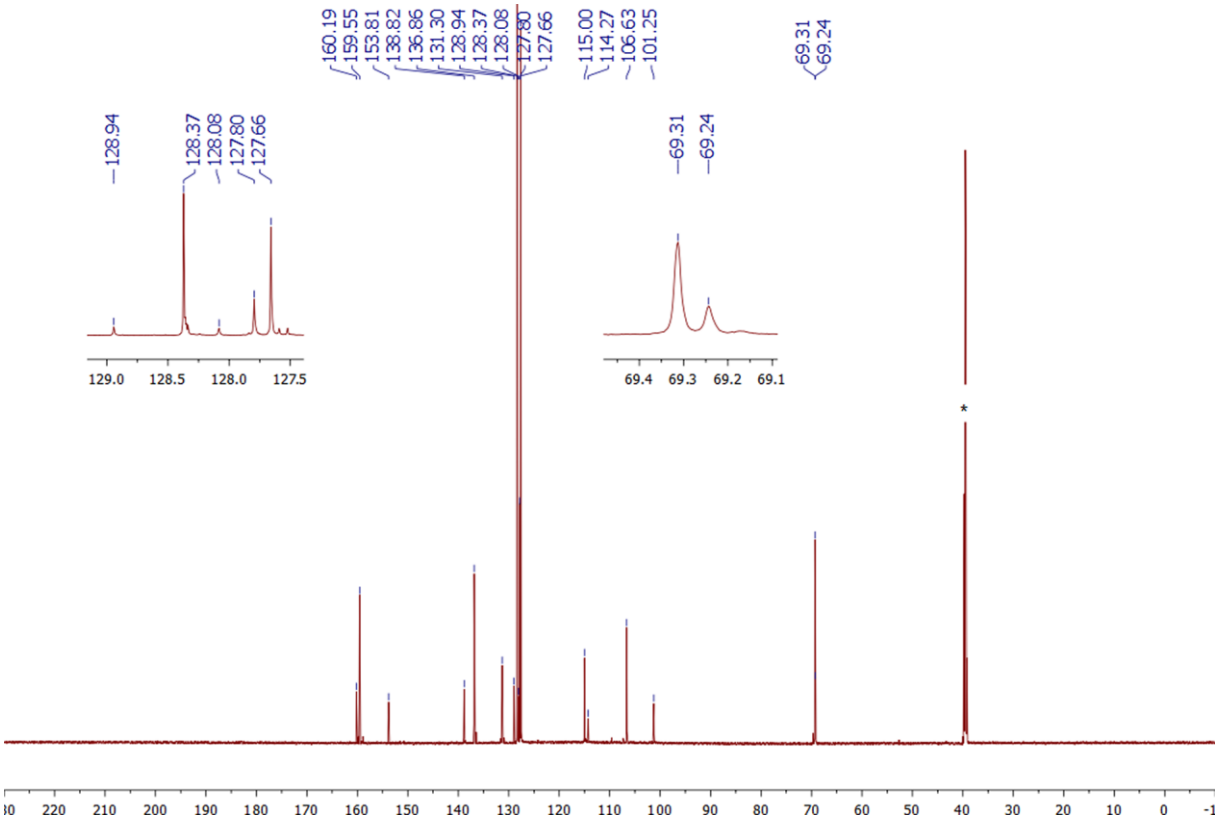

Fig. S6. [13]C NMR spectrum recorded for **5c** (201 MHz, DMSO-d_6, 298 K). The symbol * indicates DMSO-d_6 peak.

NMR data of **6**

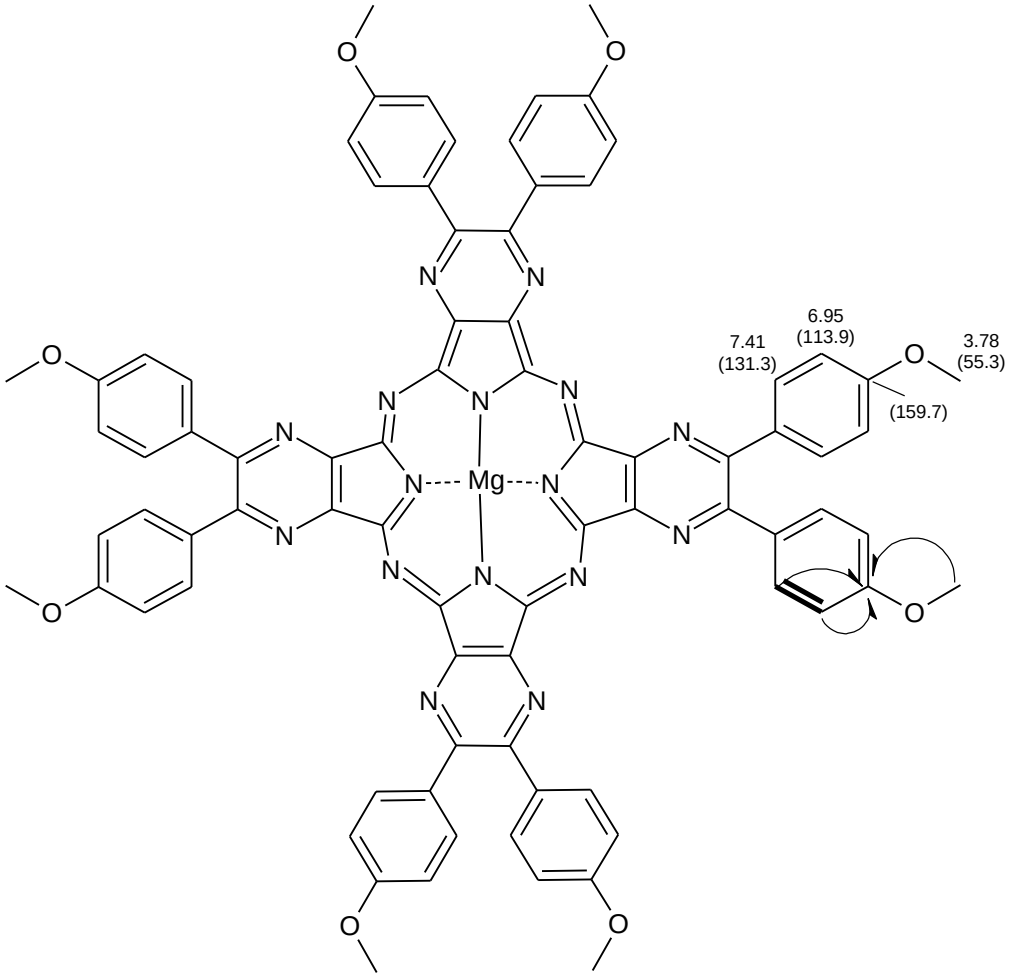

Fig. S7. ^{1}H and (^{13}C) chemical shift values [ppm] of **6**. Key ^{1}H-^{13}C HMBC and ^{1}H-^{1}H COSY correlations are marked with arrows and bold lines, respectively.

Table S3. ^{1}H and ^{13}C NMR data obtained for **6** including key correlations determined from ^{1}H-^{13}C HSQC and ^{1}H-^{13}C HMBC spectra.

δ_H (ppm)	**Multiplicity (J_{H-H} in Hz)**	**^{1}H-^{13}C HSQC δ_C (ppm)**	**^{1}H-^{13}C HMBC δ_C (ppm)**
7.41	m	131.3	159.7
6.95	m	113.9	159.7
3.78	s	55.3	159.7
Quaternary carbon atoms (ppm): 159.7			

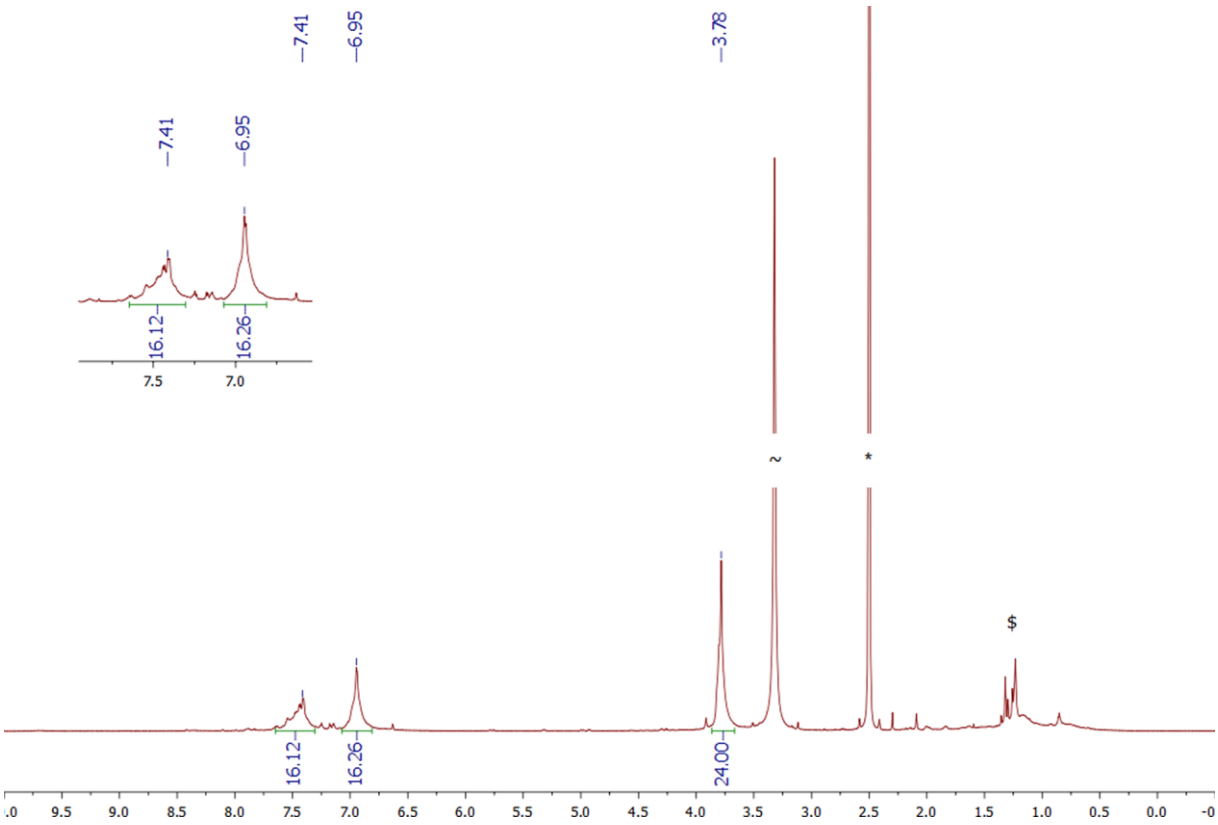

Fig. S8. [1]H NMR spectrum of **6** (800 MHz, DMSO-d_6, 298 K). The symbols *, ~ and $ indicate DMSO-d_6, water and *n*-hexane residual peaks, respectively.

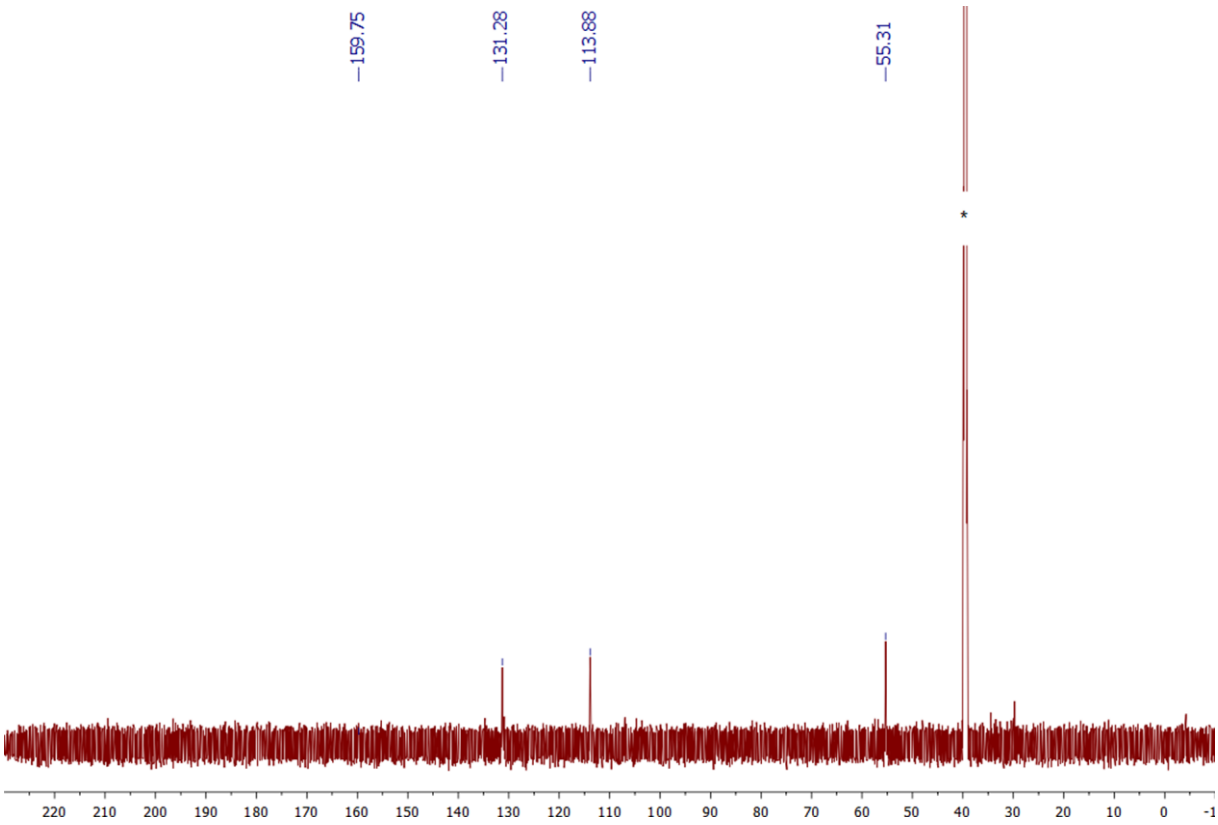

Fig. S9. [13]C NMR spectrum recorded for **6** (201 MHz, DMSO-d_6, 298 K). The symbol * indicates DMSO-d_6 peak.

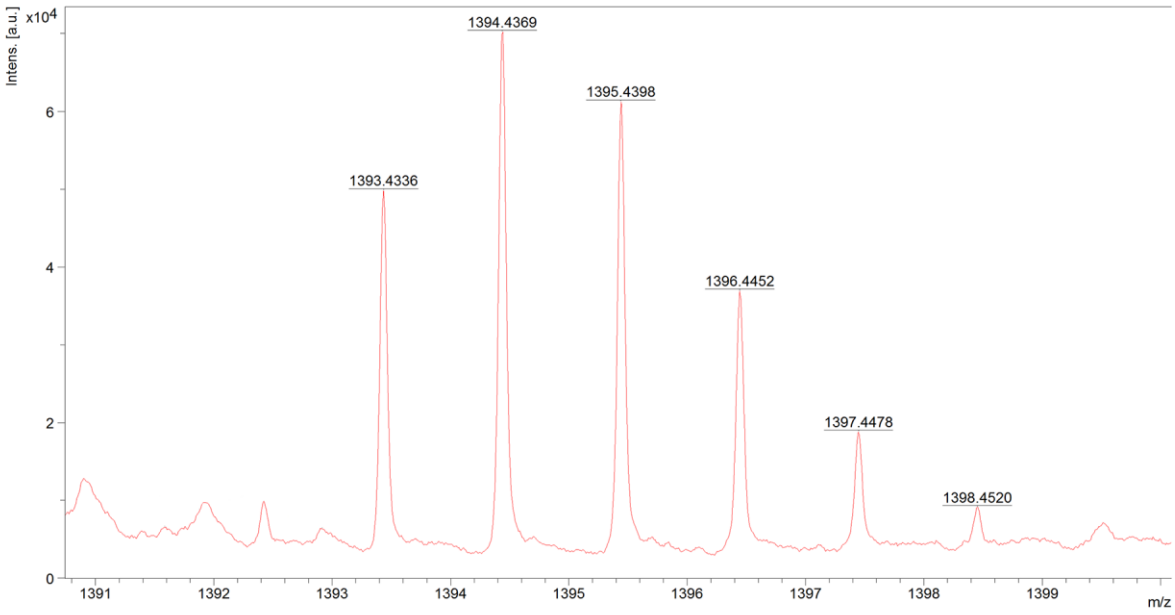

Fig. S10. MALDI-TOF HRMS spectrum of **6.** Calculated mass for $C_{80}H_{56}MgN_{16}O_8$ $[M]^+$ 1393.4345, found: *m/z* 1393.4336; for $C_{80}H_{57}MgN_{16}O_8$ $[M+H]^+$ 1394.4423, found: *m/z* 1394.4369.

NMR data of **7**

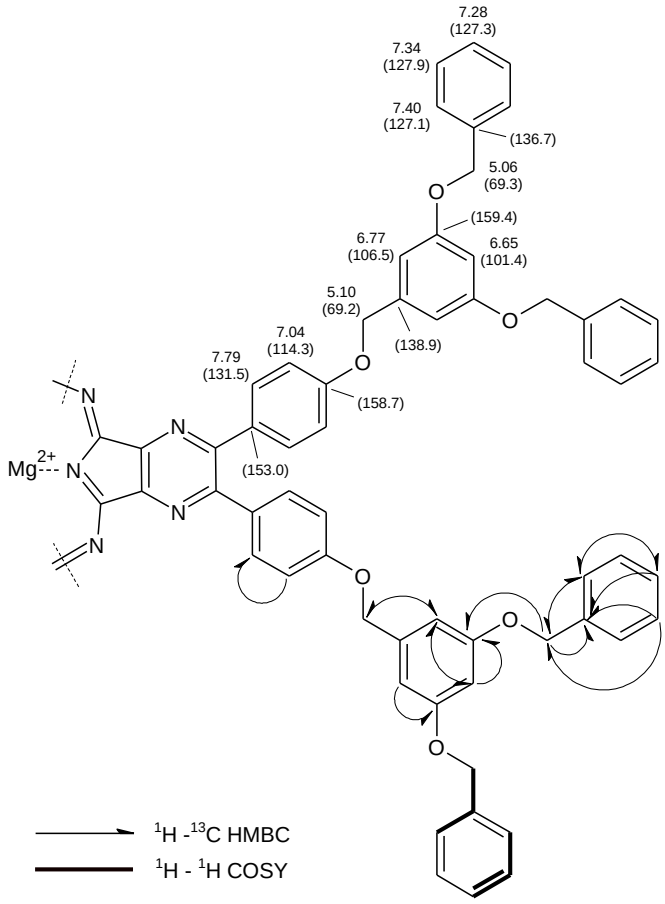

Fig. S11. ^{1}H and (^{13}C) chemical shift values [ppm] of **7**. Key ^{1}H-^{13}C HMBC and ^{1}H-^{1}H COSY correlations are marked with arrows and bold lines, respectively.

Table S4. ^{1}H and ^{13}C NMR data obtained for **7** including key correlations determined from ^{1}H-^{13}C HSQC and ^{1}H-^{13}C HMBC spectra.

δ_H (ppm)	**Multiplicity (J_{H-H} in Hz)**	**^{1}H-^{13}C HSQC δ_C (ppm)**	**^{1}H-^{13}C HMBC δ_C (ppm)**		
7.79	bs	131.5	-		
7.40	d (7.5)	127.1	127.3	69.3	
7.34	t (7.5)	127.9	136.7	69.3	
7.28	t (7.5)	127.3	136.7	127.1	
7.04	bs	114.3	131.5		
6.77	s	106.5	159.4	101.4	69.2
6.65	s	101.4	159.4	106.5	
5.10	s	69.2	106.5		
5.06	s	69.3	159.4	136.7	127.1
Other quaternary carbon atoms (ppm): 127.00, 127.8, 136.7, 138.9, 149.7, 153.0, 158.7, 159.4					

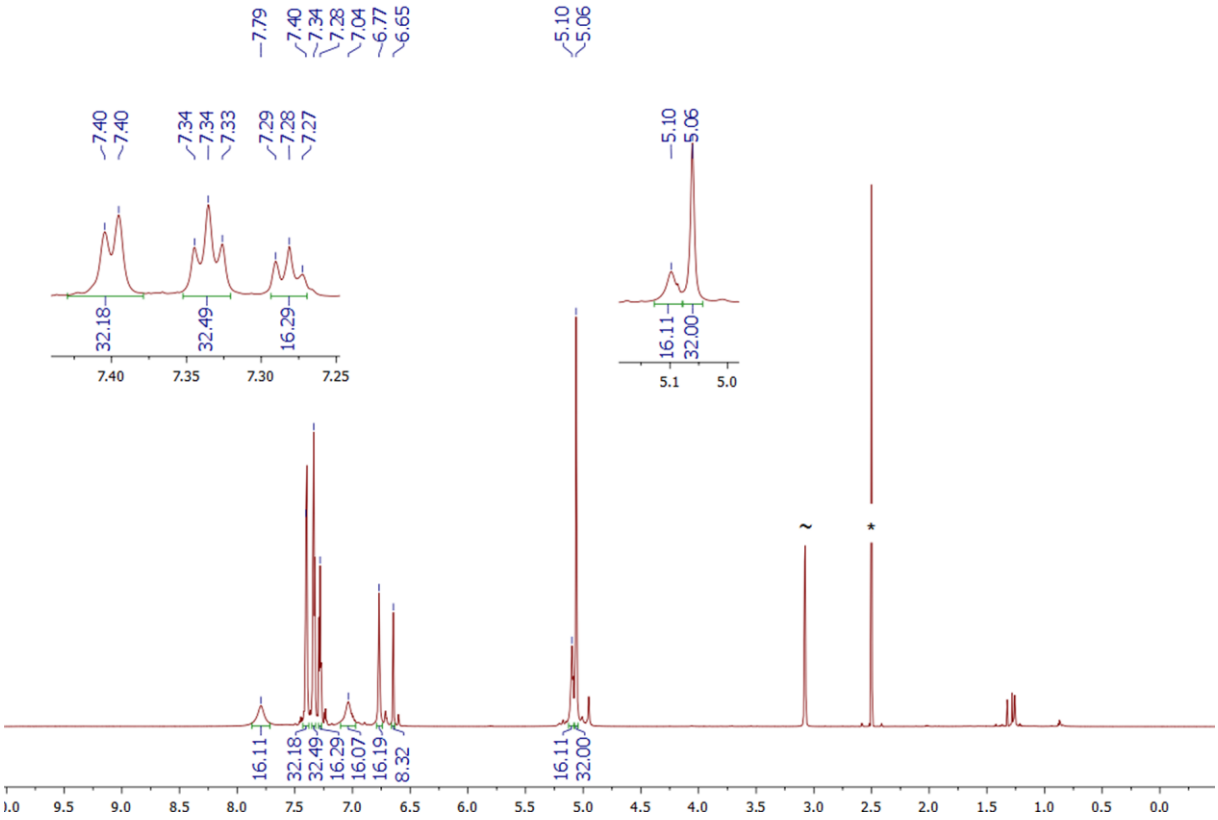

Fig. S12. [1]H NMR spectrum of **7** (800 MHz, DMSO-d_6, 353 K). The symbols * and ~ indicate DMSO-d_6 and water residual peaks, respectively.

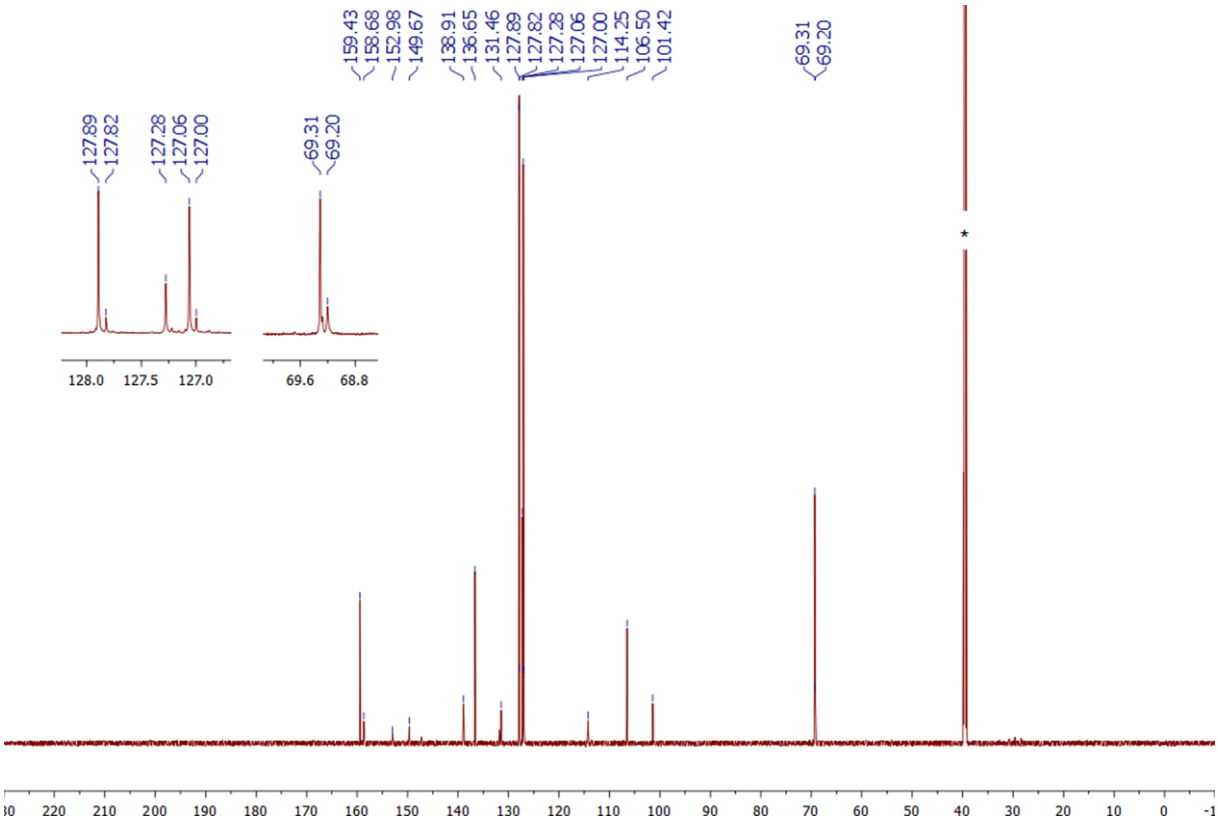

Fig. S13. [13]C NMR spectrum recorded for **7** (201 MHz, DMSO-d_6, 353 K). The symbol * indicates DMSO-d_6 peak.

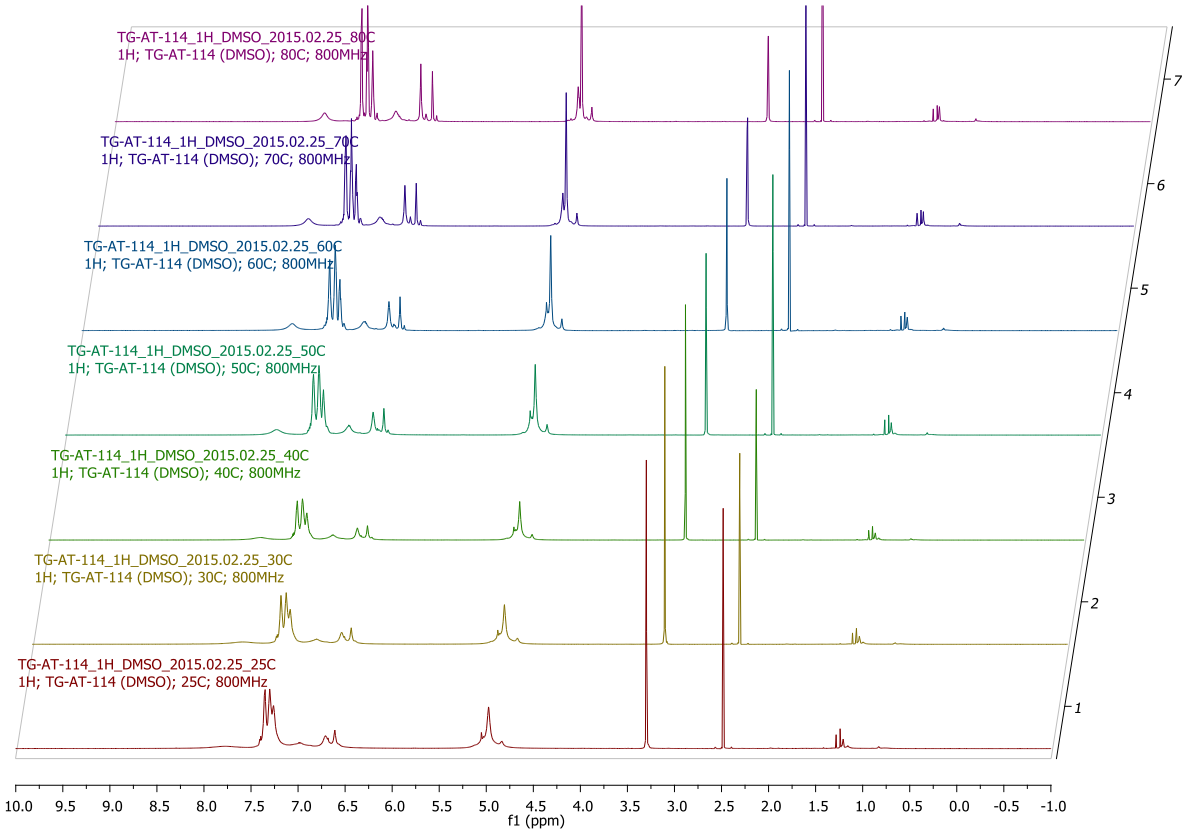

Fig. S14. ^{1}H NMR spectrum of **7** (800 MHz, DMSO-d_6). Temperature changes from 298 K (red, bottom) to 353 K (violet, top).

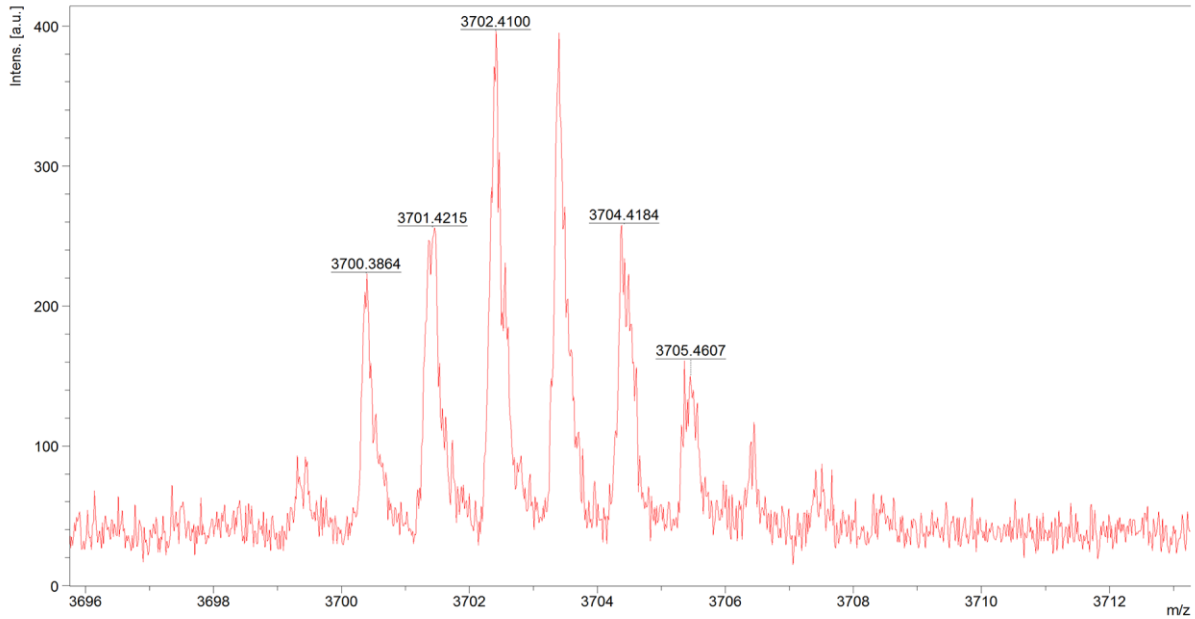

Fig. S15. MALDI-TOF HRMS spectrum of **7.** Calculated mass for $C_{240}H_{184}MgN_{16}O_{24}$ $[M]^+$ 3700.3606, found: *m/z* 3700.3864.

NMR data of **8**

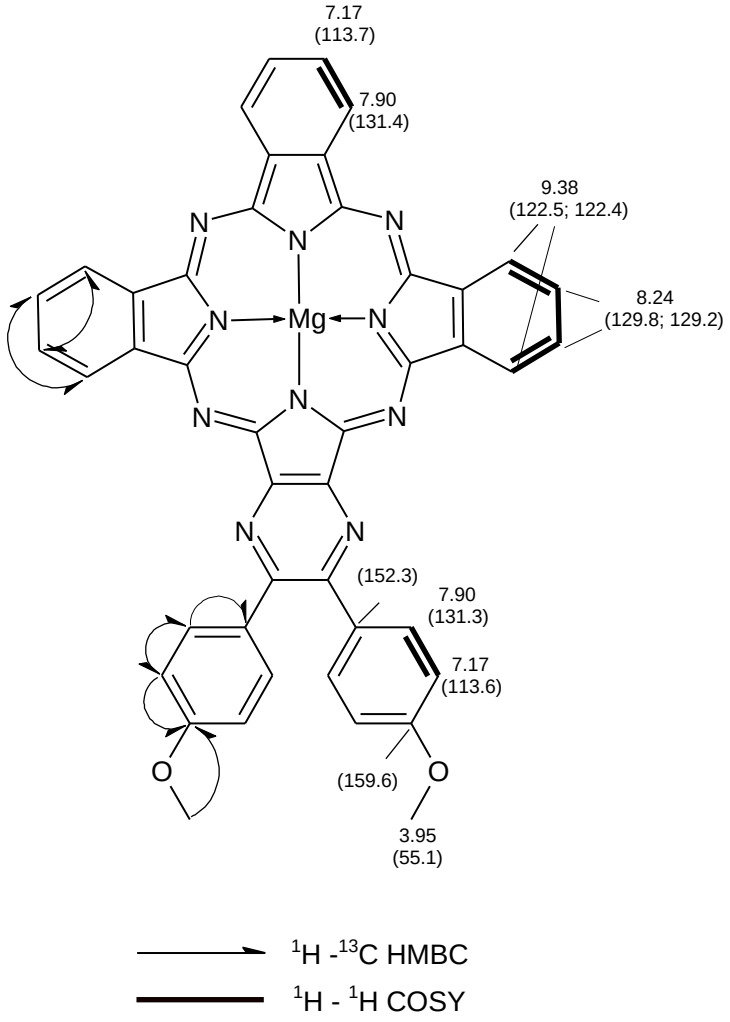

Fig. S16. ^{1}H and (^{13}C) chemical shift values [ppm] of **8**. Key ^{1}H-^{13}C HMBC and ^{1}H-^{1}H COSY correlations are marked with arrows and bold lines, respectively.

Table S5. ^{1}H and ^{13}C NMR data obtained for **8** including key correlations determined from ^{1}H-^{13}C HSQC and ^{1}H-^{13}C HMBC spectra.

δ_H (ppm)	**Multiplicity (J_{H-H} in Hz)**	**^{1}H-^{13}C HSQC δ_C (ppm)**	**^{1}H-^{13}C HMBC δ_C (ppm)**	
9.38	m	122.5	129.8	
9.38	m	122.4	129.2	
8.24	m	129.8	122.5	
8.24	m	129.2	122.4	
7.90	m	131.4	113.7	
7.90	m	131.3	152.3	113.6
7.17	m	113.7	131.4	
7.17	m	113.6	159.6	131.3
3.95	m	55.1	159.6	
Other quaternary carbon atoms (ppm): 152.3				

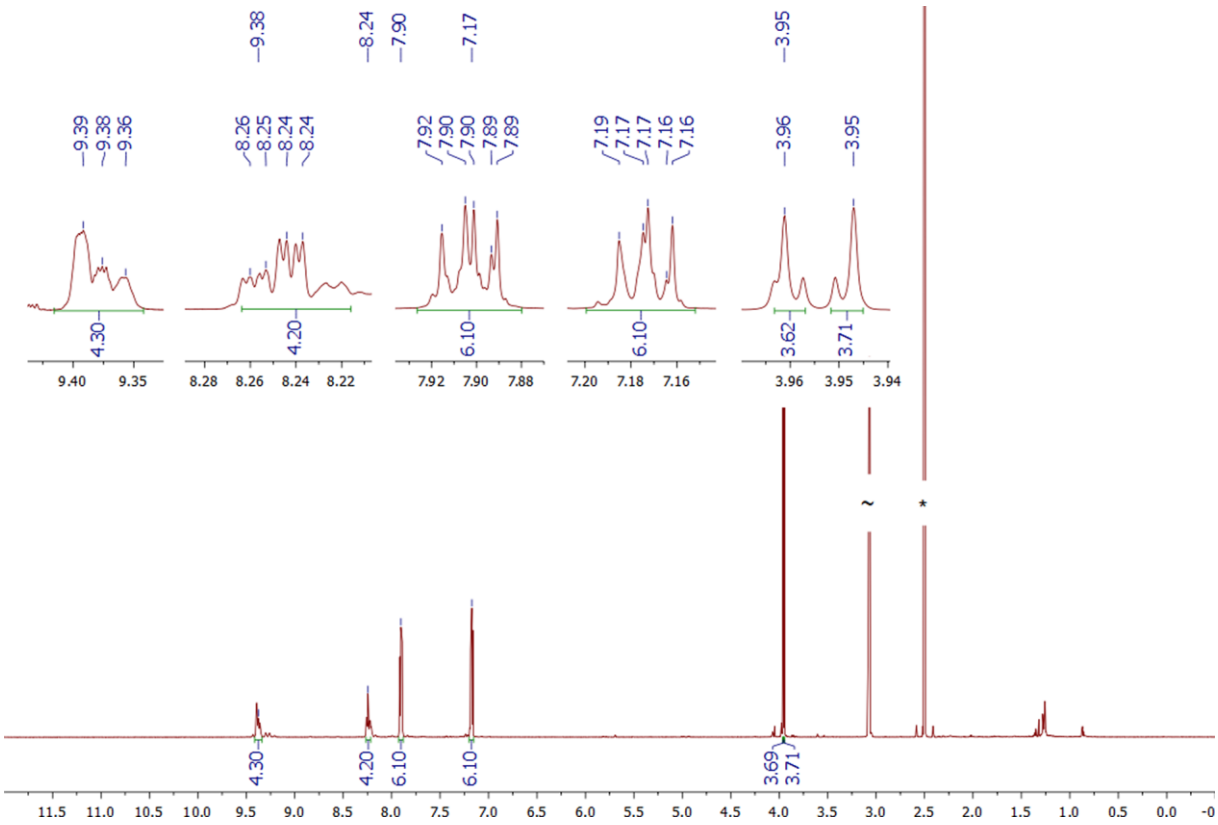

Fig. S17. [1]H NMR spectrum of **8** (800 MHz, DMSO-d_6, 353 K). The symbols * and ~ indicate DMSO-d_6 and water residual peaks, respectively.

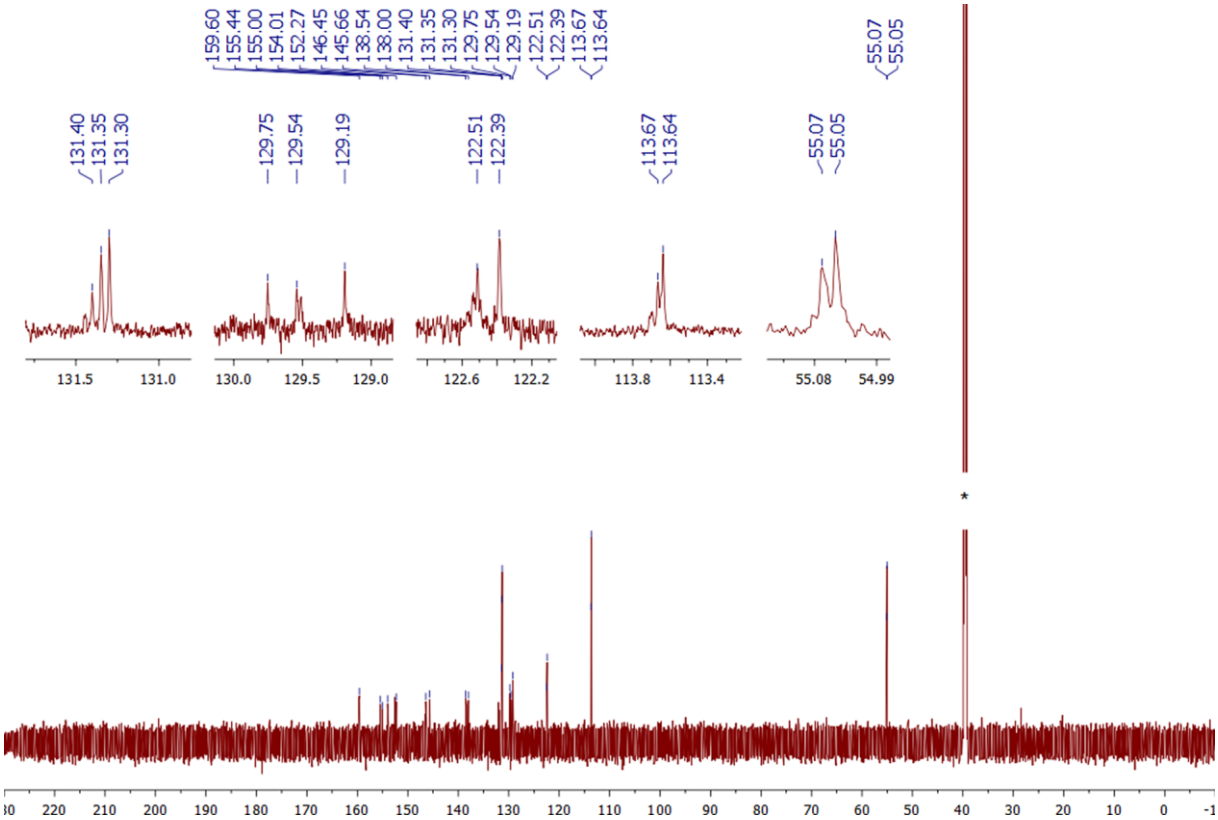

Fig. S18. [13]C NMR spectrum recorded for **8** (201 MHz, DMSO-d_6, 353 K). The symbol * indicates DMSO-d_6 peak.

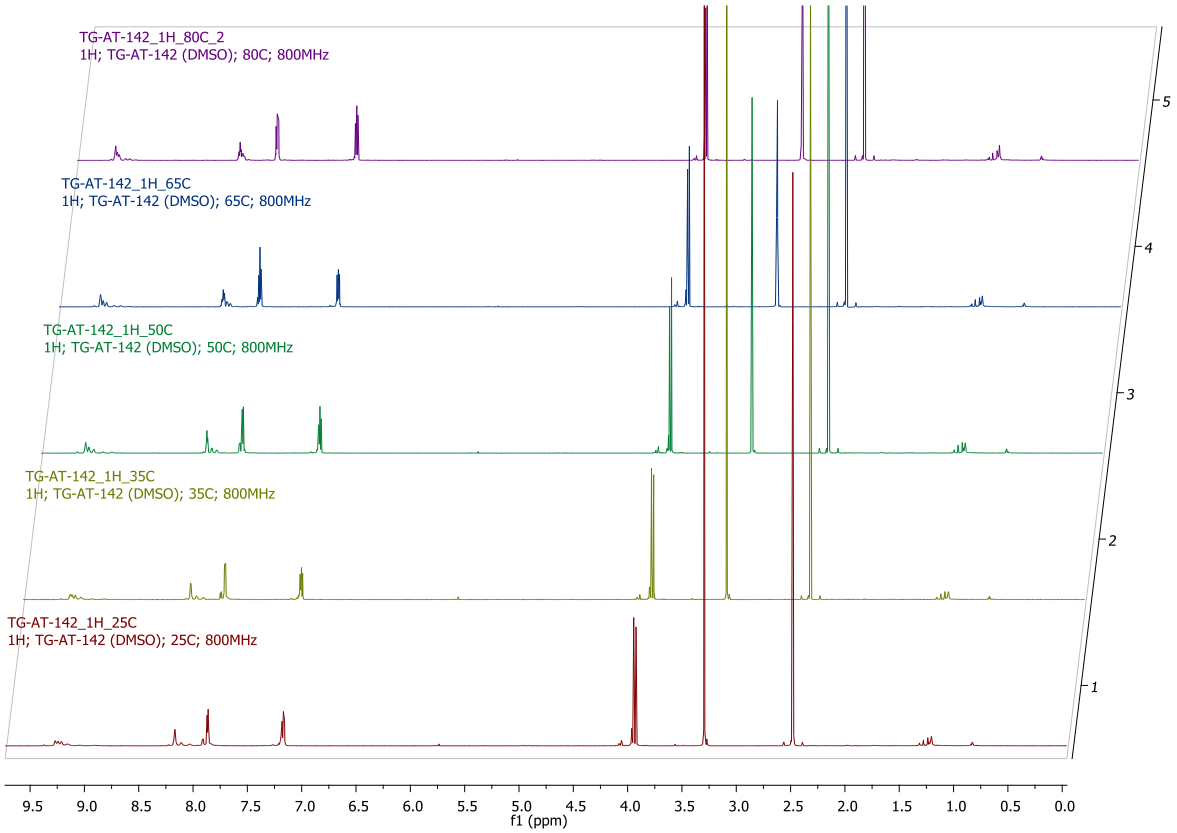

Fig S19. ^{1}H NMR spectrum of **8** (800 MHz, DMSO-d_6). Temperature changes from 298 K (red, bottom) to 353 K (violet, top). With the rise of temperature, peaks become better resolved.

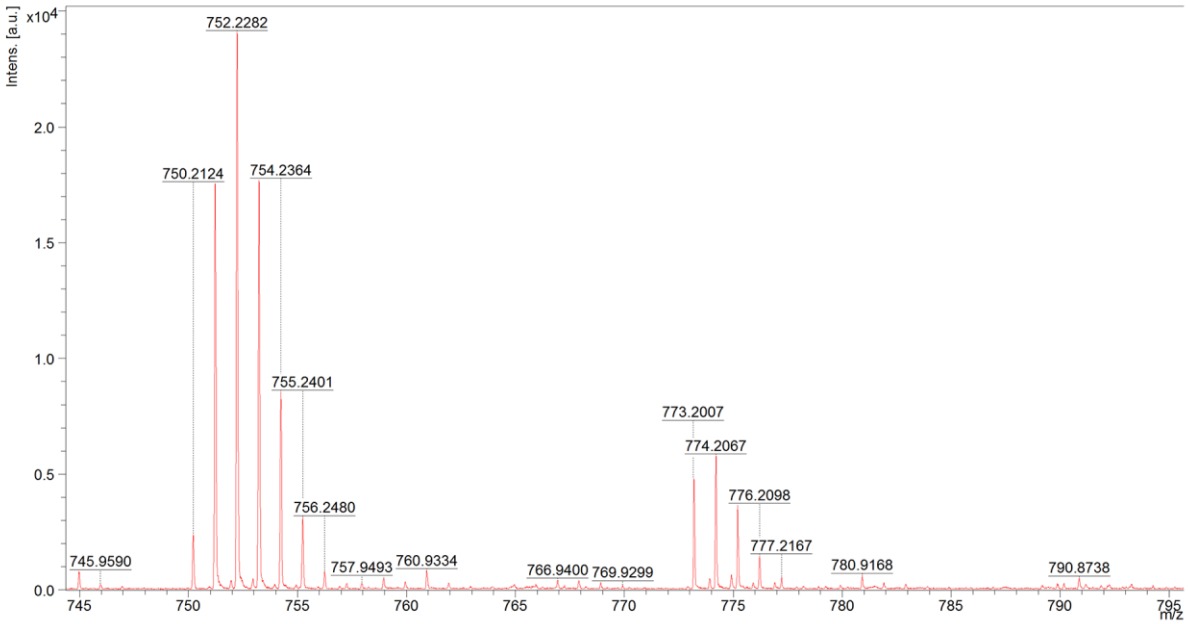

Fig. S20. MALDI-TOF HRMS spectrum of **8.** Calculated mass for $C_{44}H_{26}MgN_{10}O_2$ $[M]^+$ 750.2091, found: *m/z* 750.2124; for $C_{44}H_{26}MgN_{10}NaO_2$ $[M+Na]^+$ 773.1988, found: m/z 773.2007.

NMR data of **9**

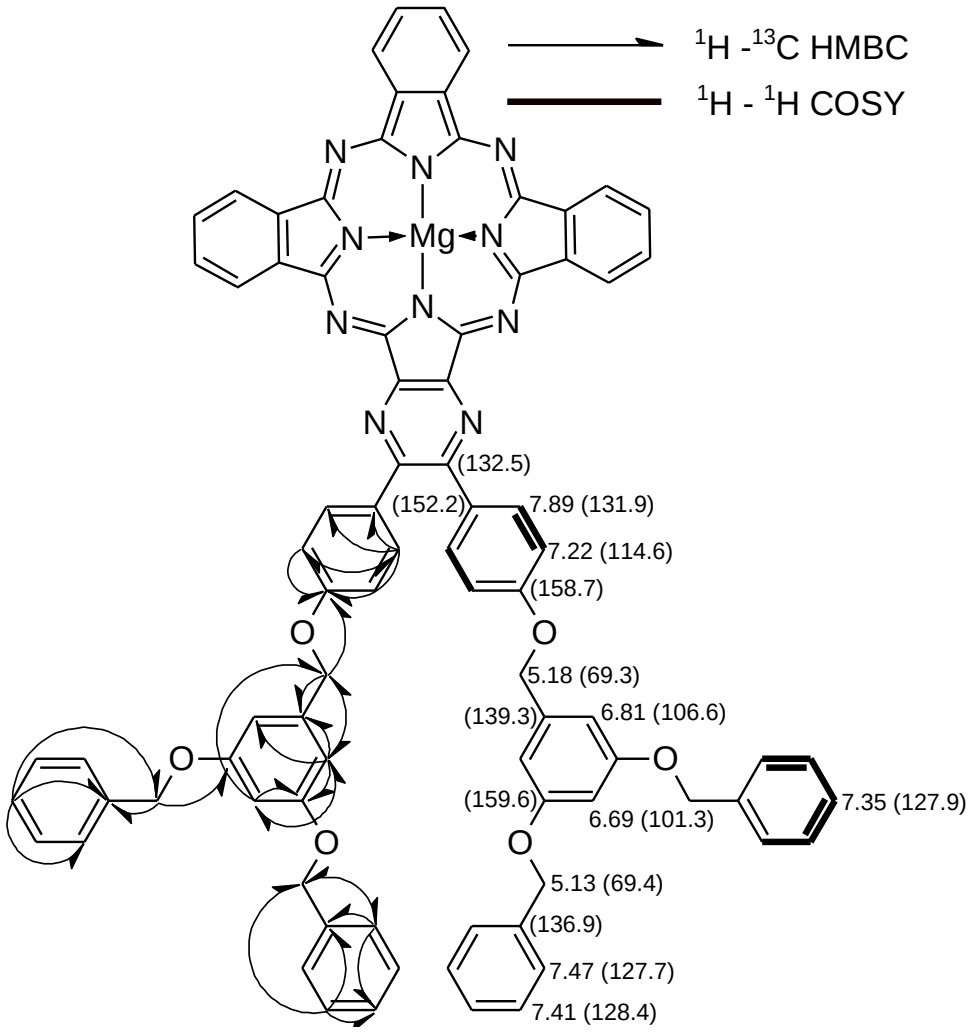

Fig. S21. ^{1}H and (^{13}C) chemical shift values [ppm] of **9**. Key ^{1}H-^{13}C HMBC and ^{1}H-^{1}H COSY correlations are marked with arrows and bold lines, respectively.

Table S6. ^{1}H and ^{13}C NMR data obtained for **9** including key correlations determined from ^{1}H-^{13}C HSQC and ^{1}H-^{13}C HMBC spectra.

δ_H (ppm)	**Multiplicity (J_{H-H} in Hz)**	**^{1}H-^{13}C HSQC δ_C (ppm)**	**^{1}H-^{13}C HMBC δ_C (ppm)**
9.13 – 8.59	m	122.5	129.4 129.2
8.09 – 7.93	m	129.4 129.2 128.4 128.3 127.9 127.7	138.0 122.5
7.89	m	131.9	158.7 152.2 131.9 114.6
7.47	m	127.7	136.9 127.9 69.4
7.41	m	128.4	136.9 128.4 69.4
7.35	m	127.9	136.9 127.7 69.4
7.22	m	114.6	158.7 132.5 114.6
6.81	m	106.6	159.6 139.3 106.6 101.3 69.3
6.69	m	101.3	159.6 106.6 69.3
5.18	s	69.3	158.7 139.3 106.6
5.13	s	69.4	159.6 136.9 127.7
Other carbon atoms (ppm): 154.7, 154.4, 153.8, 153.5, 152.4, 152.0, 145.8, 145.7, 138.5, 138.1			

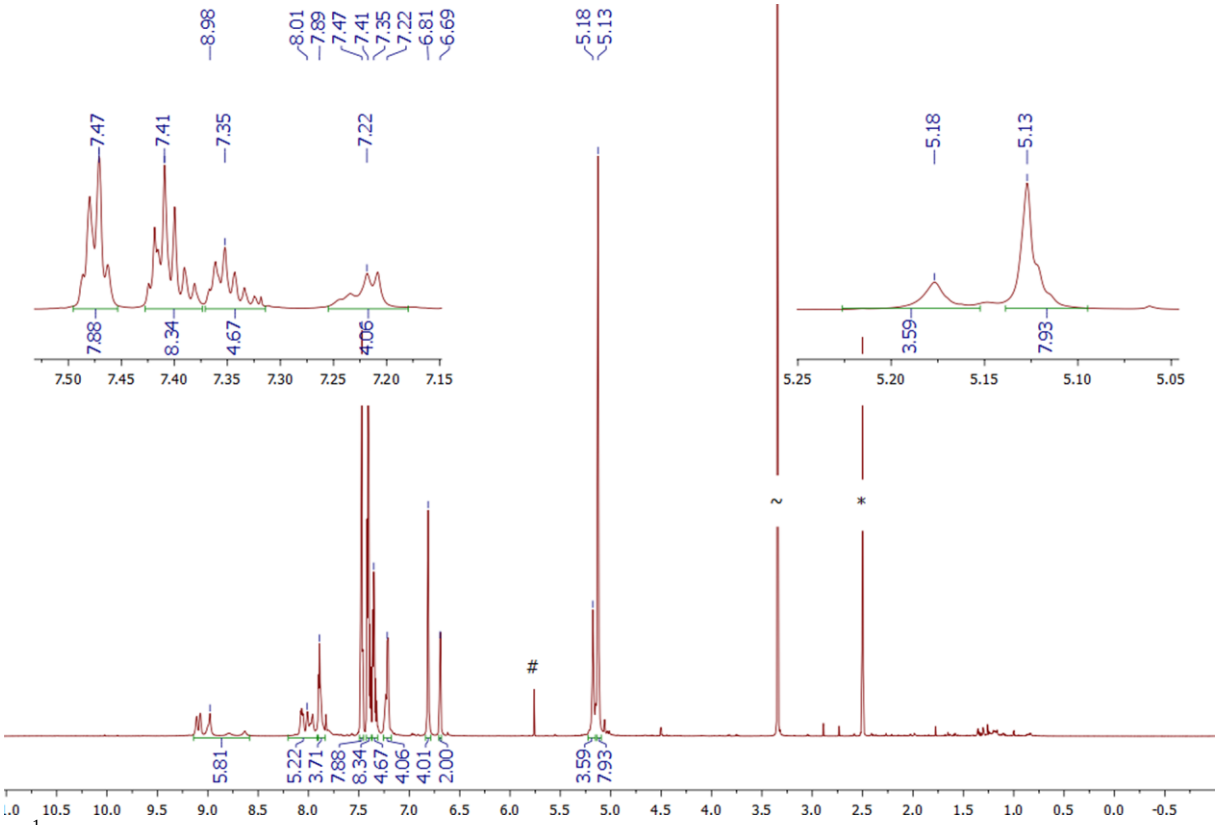

Fig. S22. ^{1}H NMR spectrum of **9** (800 MHz, DMSO-d_6, 298 K). The symbols #, ~ and * indicate CH_2Cl_2 water and DMSO-d_6 residual peaks, respectively.

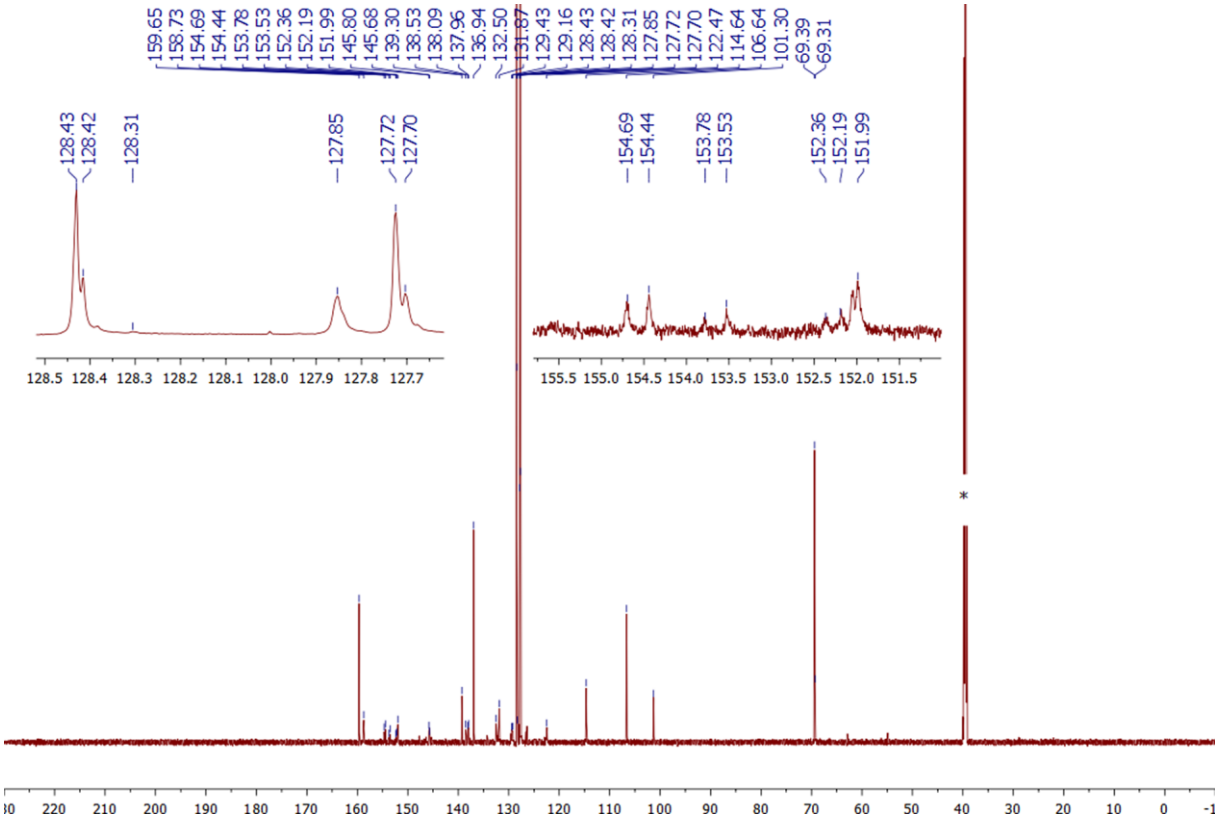

Fig. S23. ^{13}C NMR spectrum recorded for **9** (201 MHz, DMSO-d_6, 298 K). The symbol * indicates DMSO-d_6 peak.

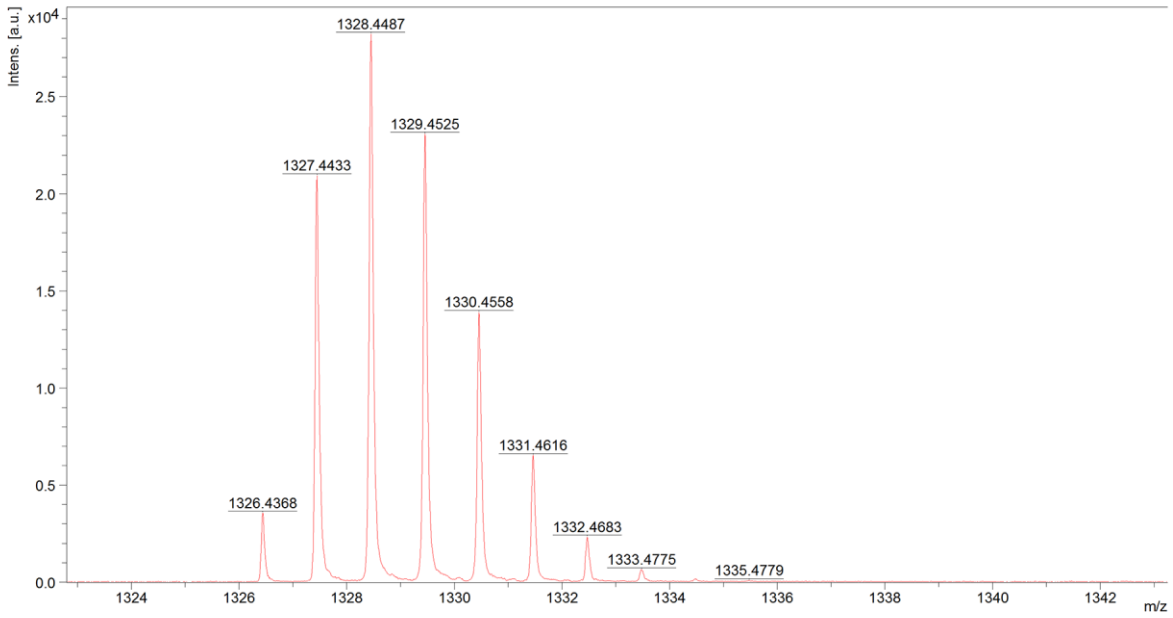

Fig. S24. MALDI-TOF HRMS spectrum of **9.** Calculated mass for $C_{84}H_{58}MgN_{10}O_6$ $[M]^+$ 1327.4420, found: *m/z* 1327.4433; for $C_{84}H_{59}MgN_{10}O_6$ $[M+H]^+$ 1328.4498, found: *m/z* 1328.4487.

X-Ray data

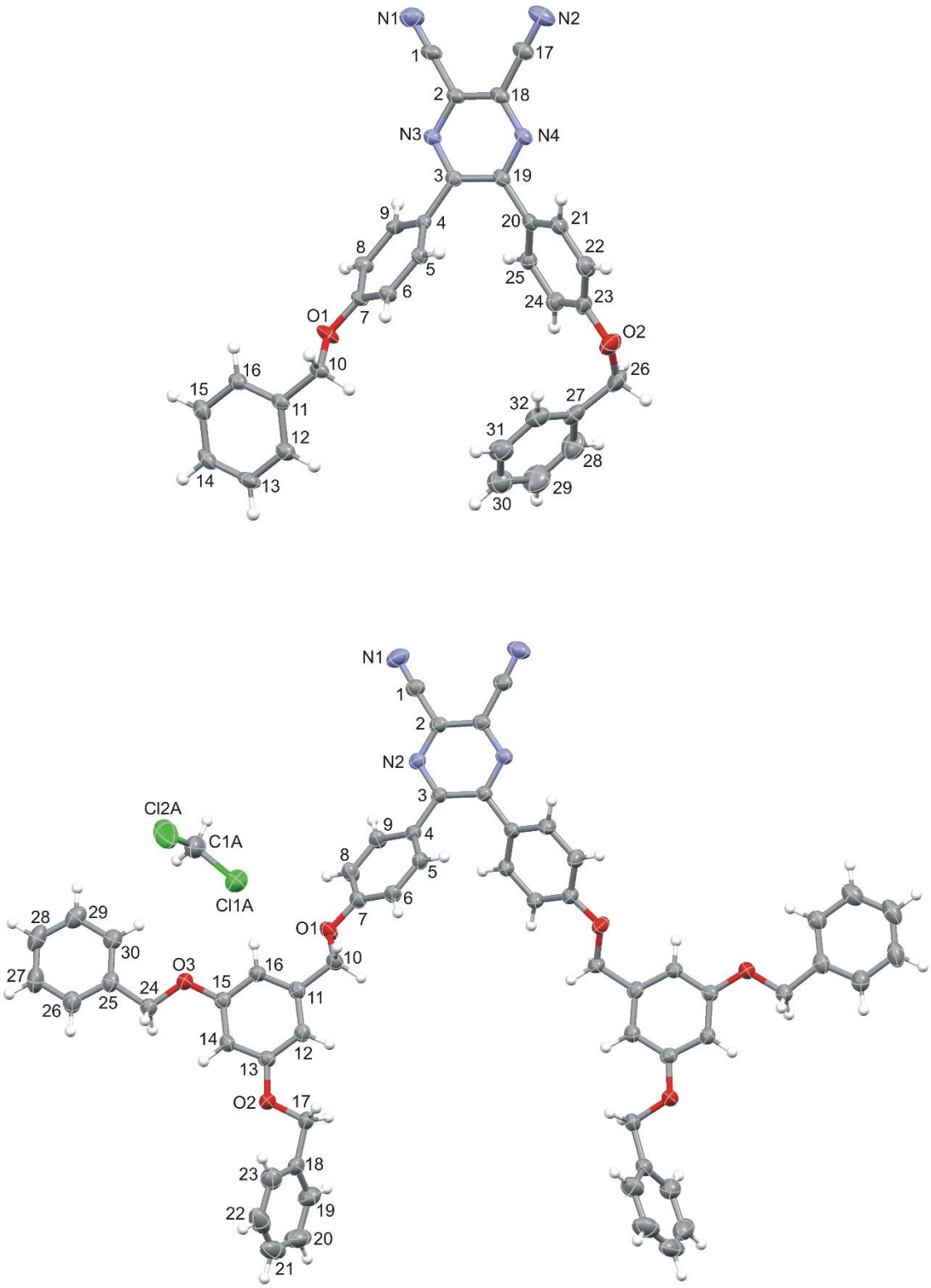

Fig. S25. Molecular structures of **5b** (top) and **5c** (botom). In **5c** only symmetry independent part of the molecule is labeled. The displacement ellipsoids are shown at the 50% of probability level.

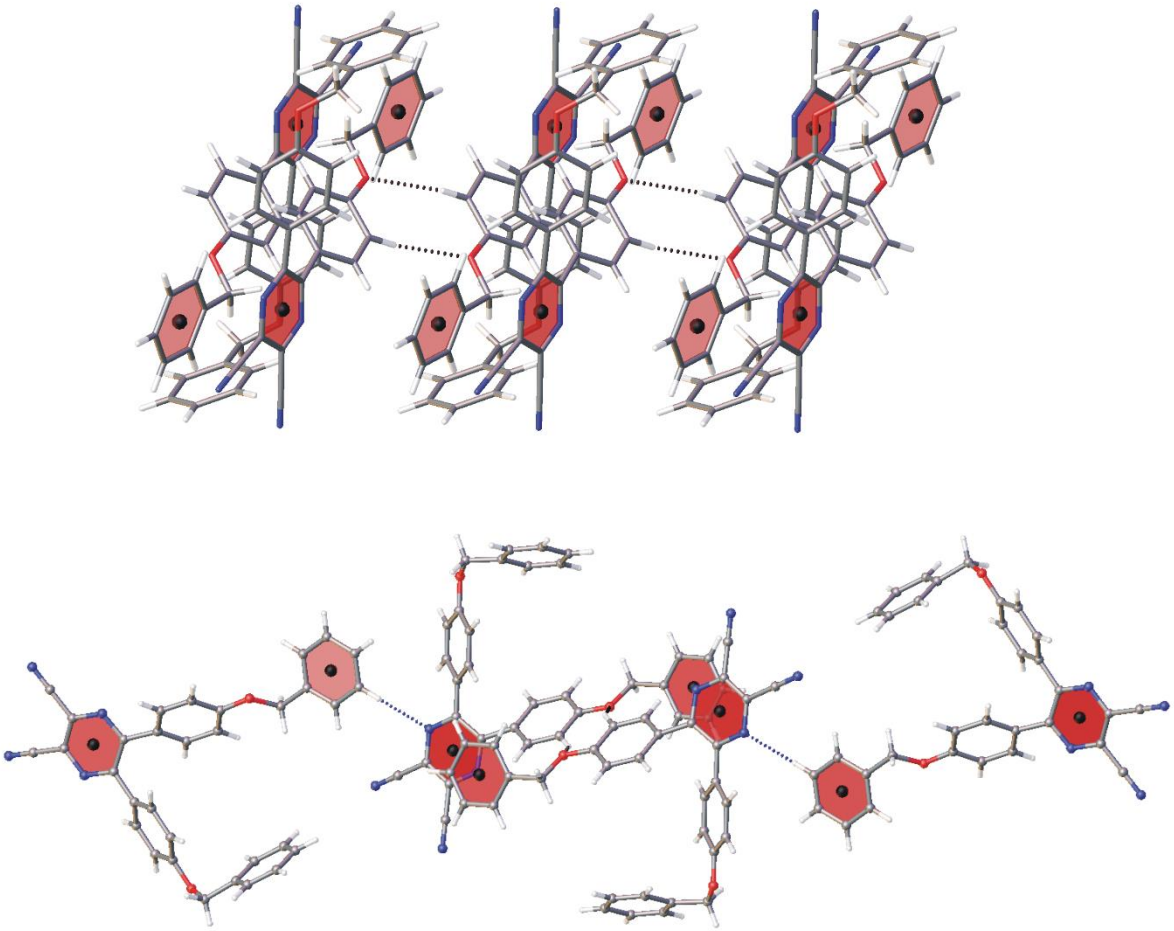

Fig. S26. C-H···O (top) and C-H···N (bottom) interactions in **5b**. Hydrogen bonds are marked as dotted lines.

Table S7. Experimental details

For all structures: $Z = 4$. Experiments were carried out at 130 K. Absorption was corrected for by multi-scan methods, *CrysAlis PRO*, Agilent Technologies, 2014. H-atom parameters were constrained.

	5b	**5c**
Crystal data		
Chemical formula	$C_{32}H_{22}N_4O_2$	$C_{60}H_{46}N_4O_6 \cdot 2(CH_2Cl_2)$
M_r	494.53	1088.86
Crystal system, space group	Monoclinic, $P2_1/n$	Monoclinic, $C2/c$
a, b, c (Å)	8.2968 (3), 11.2161 (5), 27.629 (1)	23.8249 (7), 15.5643 (4), 16.2565 (4)
β (°)	97.453 (3)	117.473 (3)
V (Å^3)	2549.38 (17)	5348.4 (3)
Radiation type	Mo $K\alpha$	Cu $K\alpha$
μ (mm^{-1})	0.08	2.47
Crystal size (mm)	0.50 × 0.30 × 0.20	0.40 × 0.20 × 0.20
Data collection		
Diffractometer	Xcalibur	SuperNova
T_{min}, T_{max}	0.991, 1.000	0.210, 1.000
No. of measured, independent and observed [$I > 2\sigma(I)$] reflections	14332, 4651, 3332	12425, 4913, 4091
R_{int}	0.038	0.043
$(\sin \theta/\lambda)_{max}$ (Å^{-1})	0.602	0.602
Refinement		
$R[F^2 > 2\sigma(F^2)]$, $wR(F^2)$, S	0.046, 0.097, 1.04	0.080, 0.249, 1.05
No. of reflections	4651	4913
No. of parameters	343	344
$\Delta\rangle_{max}$, $\Delta\rangle_{min}$ (e Å^{-3})	0.18, -0.19	0.65, -0.69

Table S8. Selected torsion angles (°) for **5b** and **5c**.

5b		**5c**	
C3—C19—C20—C25	39.9 (2)	N2—C3—C4—C9	36.6 (3)
C6—C7—O1—C10	2.2 (2)	C10—O1—C7—C6	-2.7 (4)
C11—C10—O1—C7	176.55 (14)	C7—O1—C10—C11	177.2 (2)
C19—C3—C4—C5	44.6 (2)	O1—C10—C11—C16	-37.6 (3)
C22—C23—O2—C26	-168.45 (17)	C17—O2—C13—C12	7.0 (4)
C27—C26—O2—C23	-79.9 (2)	C24—O3—C15—C16	-178.5 (2)
N3—C3—C4—C5	-132.79 (16)	C24—O3—C15—C14	1.1 (3)
N4—C19—C20—C21	38.7 (2)	C13—O2—C17—C18	177.0 (2)
O1—C10—C11—C12	128.59 (16)	O2—C17—C18—C23	-70.8 (4)
O2—C26—C27—C32	168.44 (17)	O2—C17—C18—C19	105.2 (3)
		O3—C24—C25—C26	-178.8 (2)
		O3—C24—C25—C30	2.8 (4)

Table S9. Dihedral angles (º) between the best planes of aromatic rings in **5b** and **5c**.

5b			
pyrazine/ring A	45.00(6)	pyrazine/ring C	39.12 (7)
pyrazine/ring B	6.24(8)	pyrazine/ring D	76.67(6)
5c			
pyrazine/ring A	39.7(1)	pyrazine/ring B1	3.7(2)
pyrazine/ring B	0.6(2)	pyrazine/ring B2	68.1(1)
ring B/ring B1	3.5 (2)	ring B/ring B2	67.5 (1)

Table S10. Hydrogen-bond parameters for **5b**.

D—H···*A*	*D*—H (Å)	H···*A* (Å)	*D*···*A* (Å)	*D*—H···*A* (°)
C8—H8···O1^{i}	0.95	2.50	3.3391 (19)	147.0
C22—H22···N2^{iii}	0.95	2.68	3.382 (2)	131.2

Symmetry code(s): (i) -*x*, -*y*+1, -*z*+1; (ii) *x*-1/2, -*y*+1/2, *z*+1/2; (iii) -*x*+3/2, *y*-1/2, -*z*+1/2.

HPLC analysis of purity

Porphyrazine 7

The chromatographic separation was achieved on an octadecylsilane coated column, 150 mm × 4.6 mm, 5 μm (Eclipse XDB-C18, Agilent), using phase system indicated below, at a flow rate of 1.0 mL/min

time [min]	MeOH	THF	CH_2Cl_2
0	50	20	30
5	50	20	30
8	20	50	30
15	20	50	30

assay 99.4% measured at λ = 650 nm

95% measured at λ = 343 nm

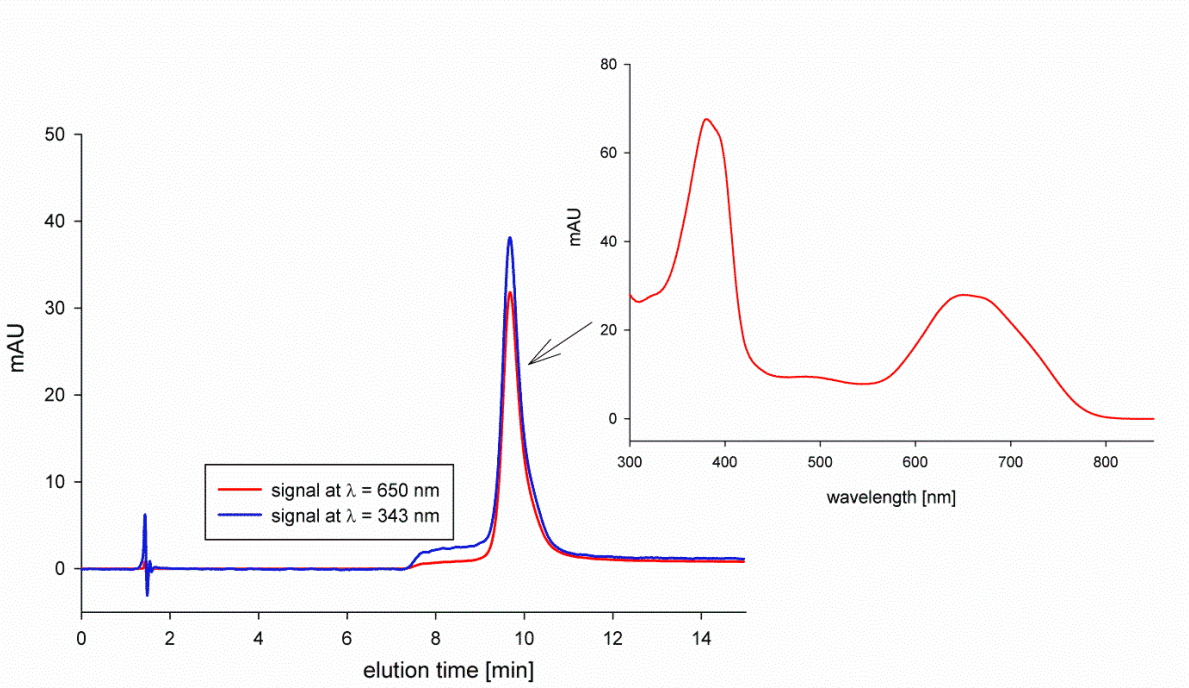

Fig. S27. Chromatogram and UV-vis spectrum of **7**.

Porphyrazine 9

The chromatographic separation was achieved on an octadecylsilane coated column, 150 mm × 4.6 mm, 5 µm (Eclipse XDB-C18, Agilent), using isocratic elution conditions, at a flow rate of 1.0 mL/min (elution conditions MeOH 55%; THF 15%;CH_2Cl_2 30%)

assay 100% measured at λ = 678 nm

94% measured at λ = 343 nm

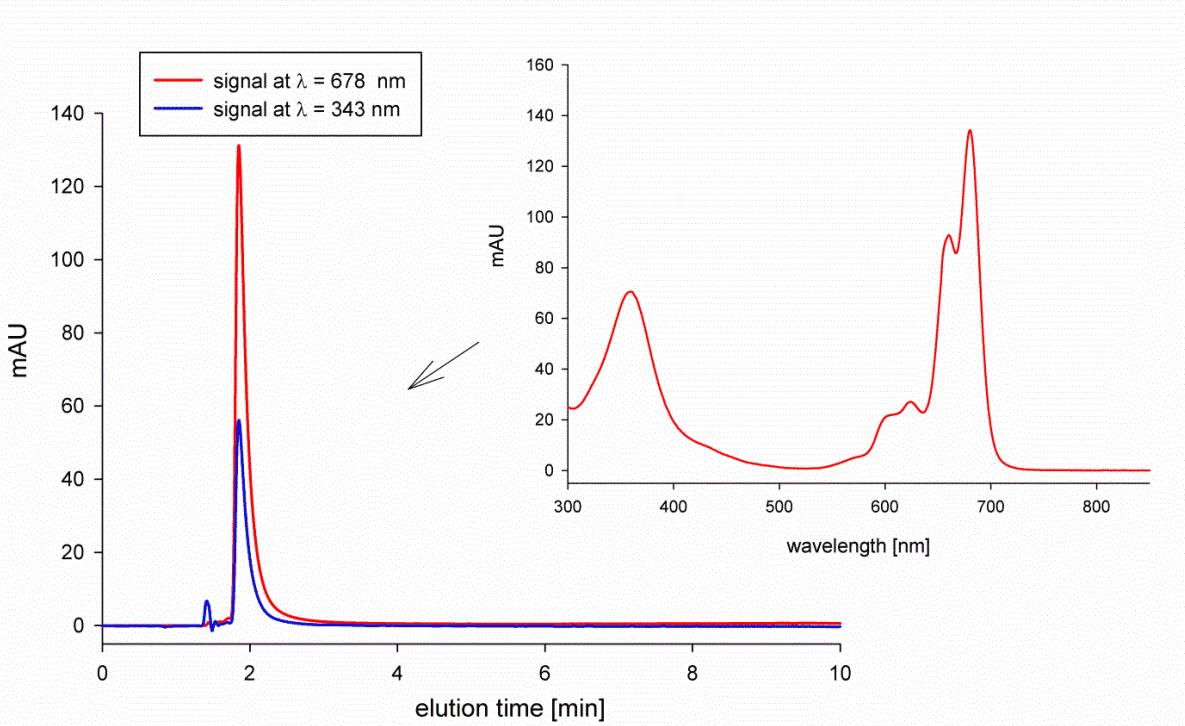

Fig. S28. Chromatogram and UV-vis spectrum of **9**.

Aggregation study

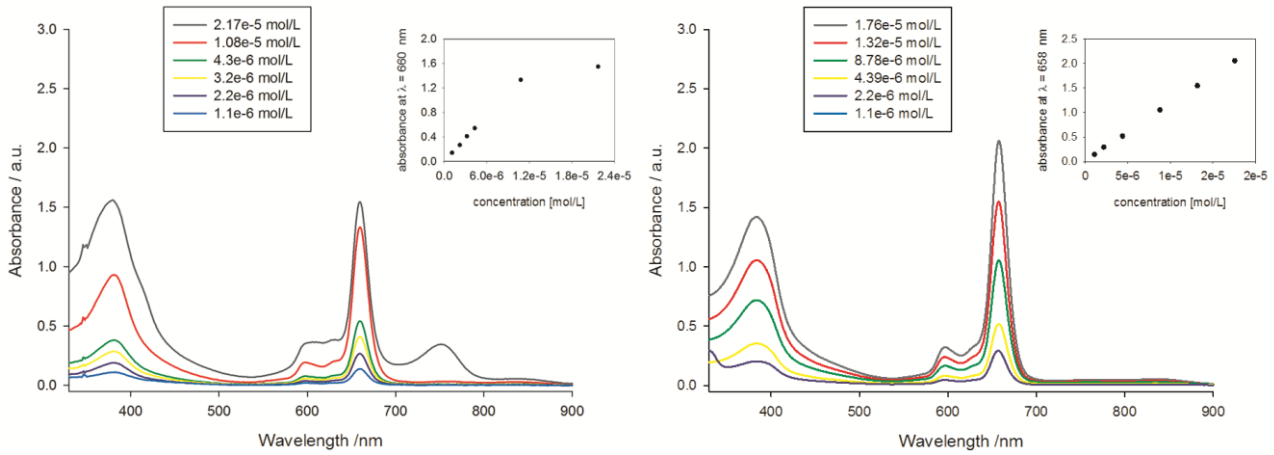

Fig. S29. UV-Vis absorption spectra of **6** in DMF (left) and DMSO (right). Inset presents a correlation between absorbance and concentration.

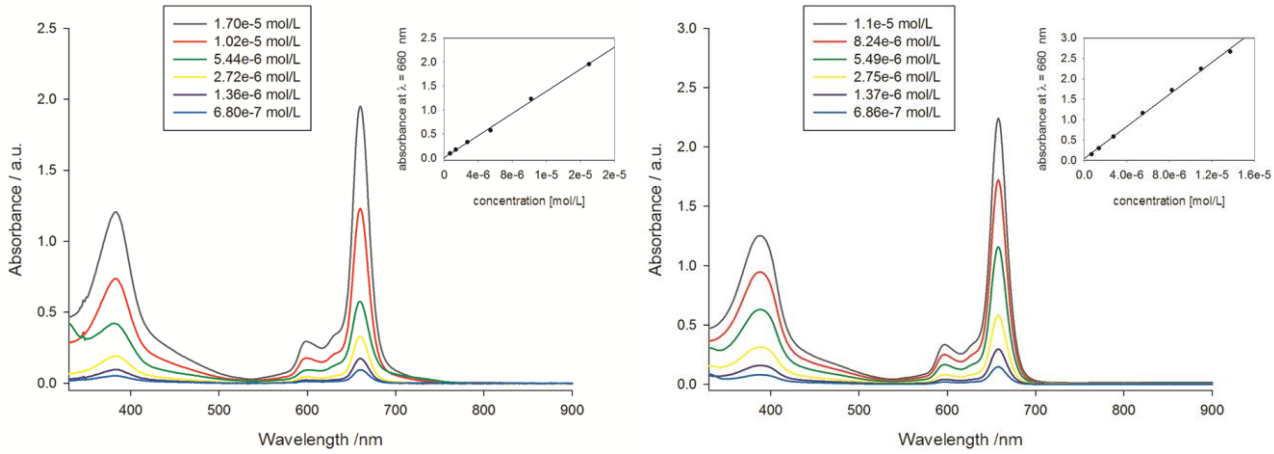

Fig. S30. UV-Vis absorption spectra of **7** in DMF (left) and DMSO (right). Inset presents a correlation between absorbance and concentration.

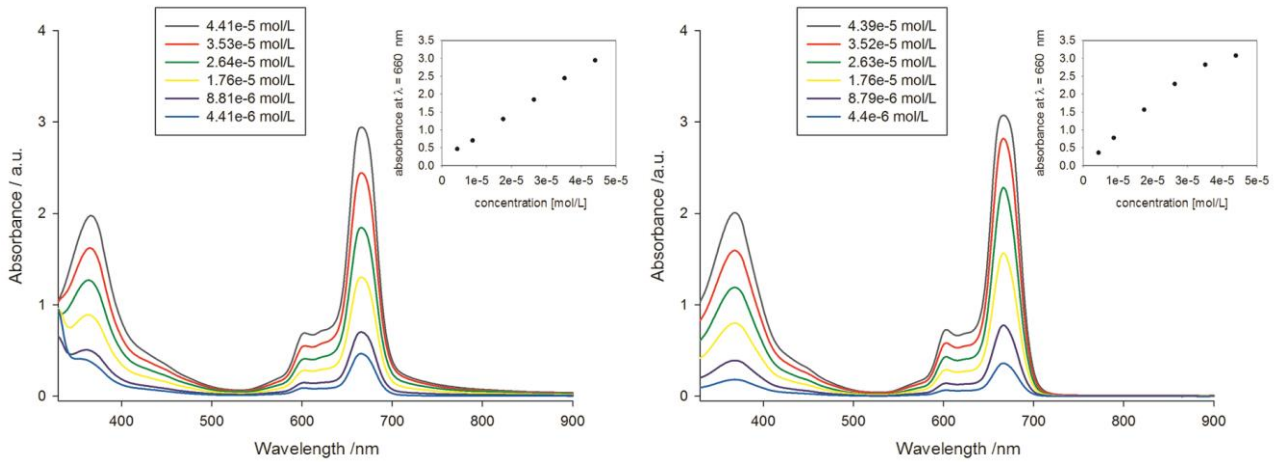

Fig. S31. UV-Vis absorption spectra of **8** in DMF (left) and DMSO (right). Inset presents a correlation between absorbance and concentration.

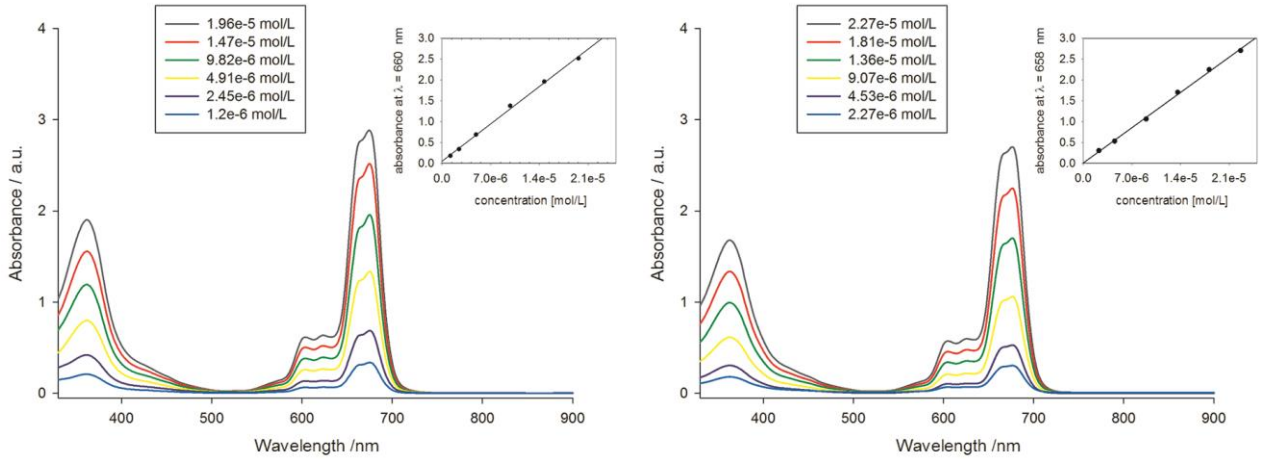

Fig. S32. UV-Vis absorption spectra of **9** in DMF (left) and DMSO (right). Inset presents a correlation between absorbance and concentration.

Table S11. Statistical parameters of absorbance vs. concentration linear regression in DMF.

Compound	DMF										
	a	Δa	b	Δb	Sa	Sb	ta	t_b	tα,f	r	n
6	70175.457	32537.798	0.199	0.332	12655.542	0.129	5.545	**1.542**	**2.571**	**0.941**	6
7	114900.239	7215.501	0.00881	0.061	2806.496	0.0238	40.941	**0.369**	**2.571**	**0.999**	6
8	63404.083	2084.188	0.172	0.056	810.653	0.0217	78.214	**7.952**	**2.571**	**1.000**	6
9	128087.450	7492.866	0.0495	0.083	2914.378	0.0322	43.950	**1.538**	**2.571**	**0.999**	6

Table S12. Statistical parameters of absorbance vs. concentration linear regression in DMSO.

Compound	DMSO										
	a	Δa	b	Δb	Sa	Sb	ta	t_b	tα,f	r	n
6	115800.395	2199.781	0.024	0.022	855.613	0.008	135.342	**2.834**	**2.571**	**1.000**	6
7	204248.508	5013.118	0.02	0.031	1949.871	0.012	104.750	**1.627**	**2.571**	**1.000**	6
8	70887.836	14958.811	0.203	0.399	5818.285	0.155	12.184	**1.308**	**2.571**	**0.987**	6
9	120748.114	7203.957	0.009	0.099	2802.006	0.039	43.093	**0.238**	**2.571**	**0.999**	6

Singlet oxygen measurements

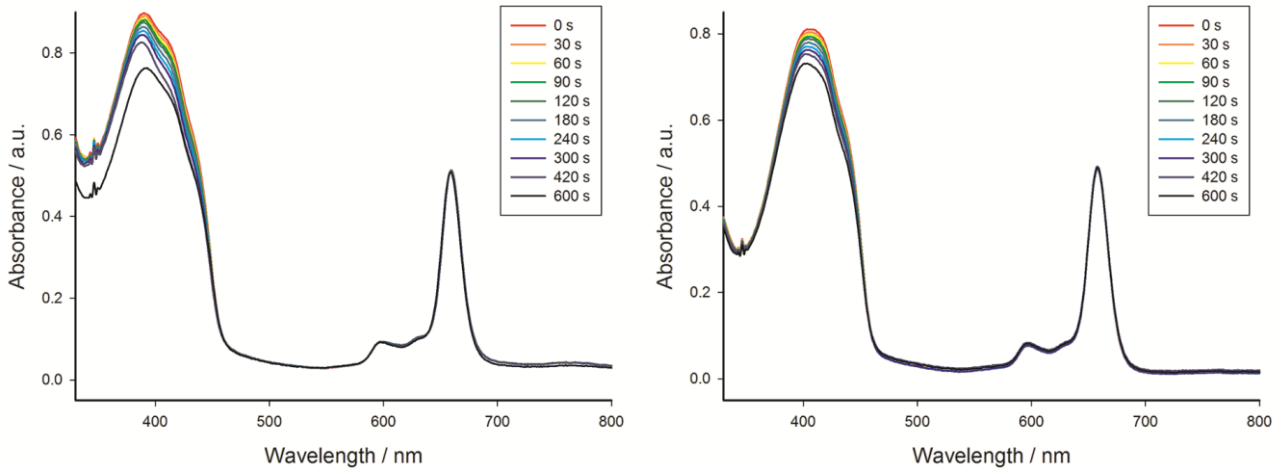

Fig. S33. Changes in the UV–vis spectra of DPBF and **6** in DMF (left) and DMSO (right) during irradiation at Q-band.

.

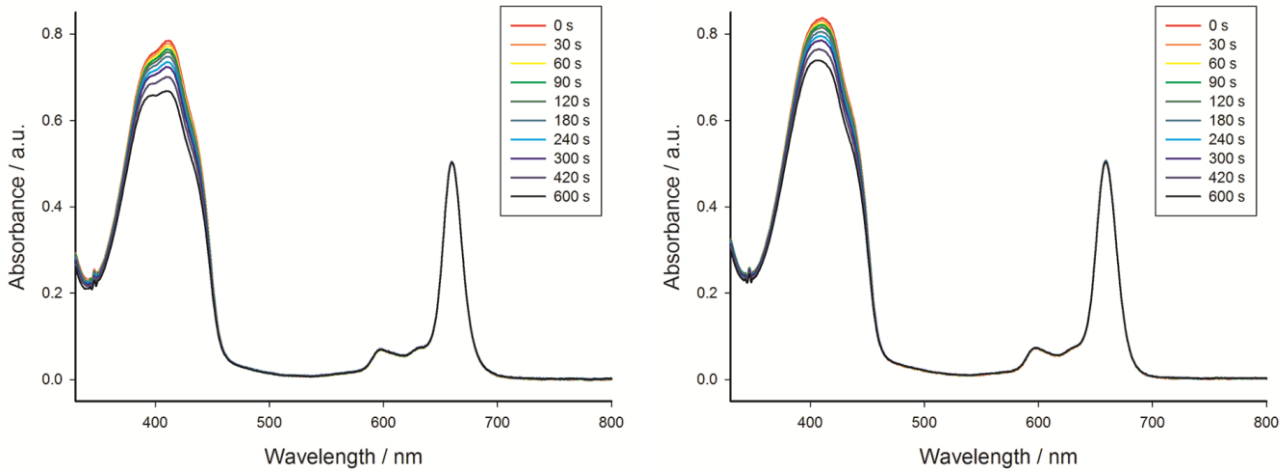

Fig. S34. Changes in the UV–vis spectra of DPBF and **7** in DMF (left) and DMSO (right) during irradiation at Q-band.

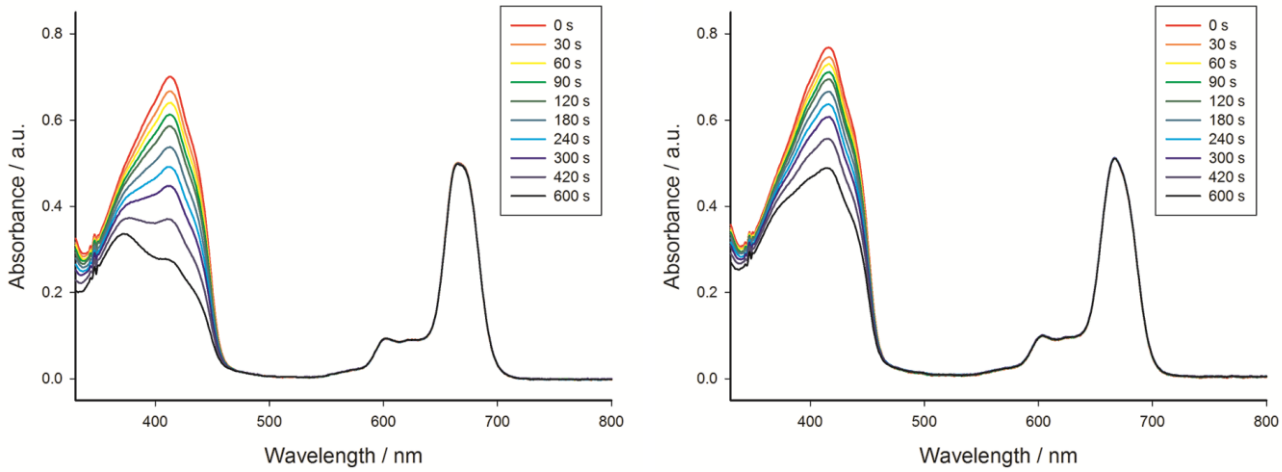

Fig. S35. Changes in the UV–vis spectra of DPBF and **8** in DMF (left) and DMSO (right) during irradiation at Q-band.

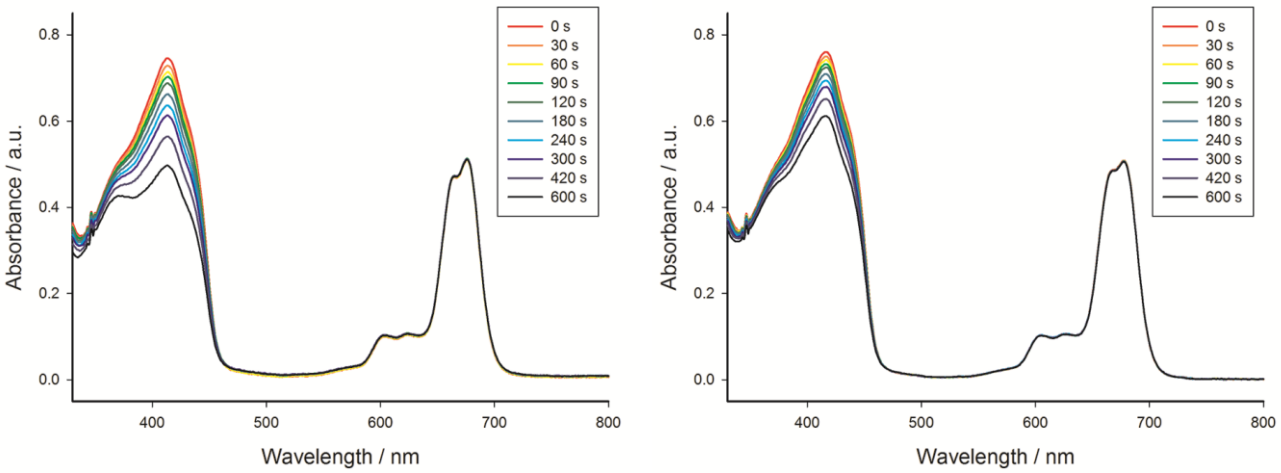

Fig. S36. Changes in the UV–vis spectra of DPBF and **9** in DMF (left) and DMSO (right) during irradiation at Q-band.

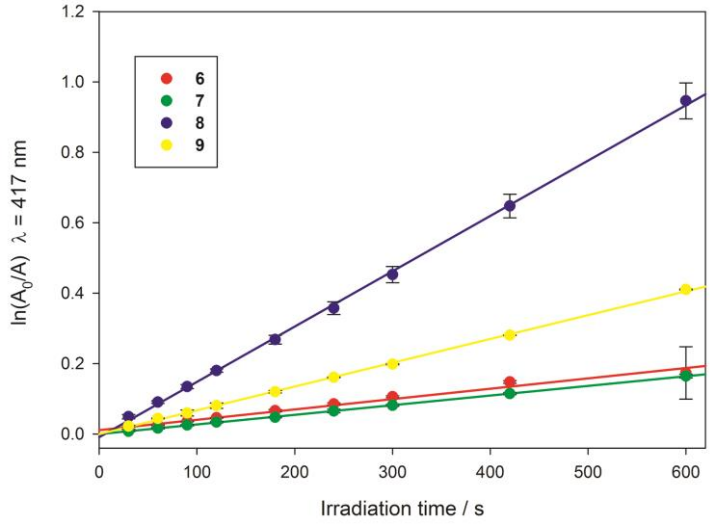

Fig. S37. First-order plots for the oxidation of diphenylisobenzofuran (DPBF) during irradiation of porphyrazine/DPBF solutions in DMF.

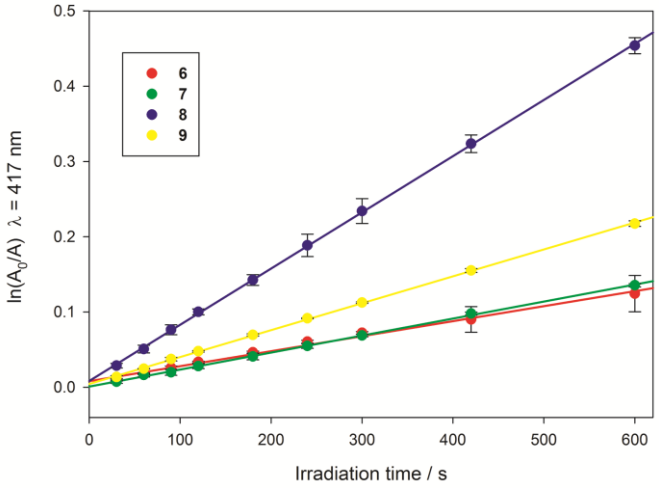

Fig. S38. First-order plots for the oxidation of diphenylisobenzofuran (DPBF) during irradiation of porphyrazine/DPBF solutions in DMSO.

Fluorescence spectra

Steady state fluorescence quantum yields were measured in solutions, using JASCO FP-6200 and 1 cm-thick-cells. Absorbance of the solution was kept below 0.1 at the maximum of Q-band, in order to avoid reabsorption of the emitted fluorescence.

Quantum yields were calculated according to equation:

$$\Phi_F = \Phi_F^{st} \frac{\int F_X\left(1 - 10^{-A_{st}}\right)}{\int F_{st}\left(1 - 10^{-A_X}\right)} \frac{(n_X)^2}{(n_{st})^2}$$

Here, $\int F_X$ is the area under the emission curve of the sample, $\int F_{st}$ is the area under the emission curve of the standard, A_X and A_{st} are the absorbance of the sample and standard at the excitation wavelength, respectively. n_X is the solvent refractive index for the sample, n_{st} the solvent refractive index for the standard and Φ^{st}_F is the value of the fluorescence quantum yield of the standard. Zinc(II) pthtalocyanine was used as a standard, excitation wavelength was λ = 600 nm.

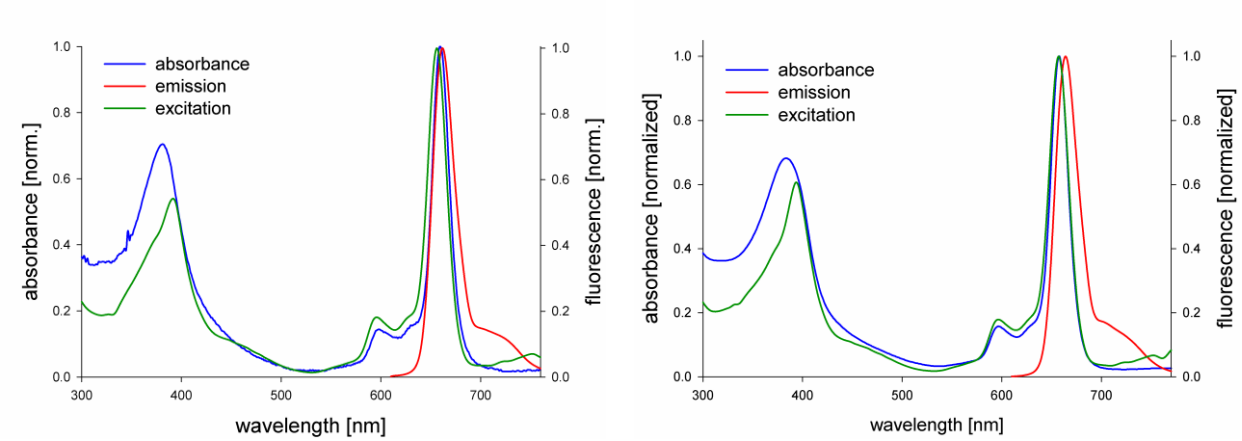

Fig. S39. Absorbance, emission and excitation spectra of **6** in DMF (left) and DMSO (right).

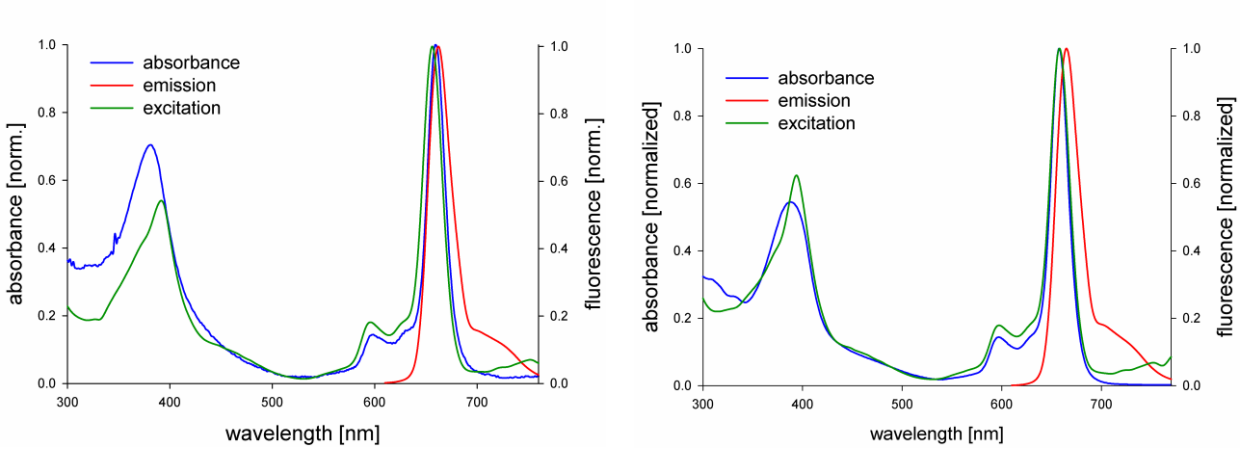

Fig. S40. Absorbance, emission and excitation spectra of **7** in DMF (left) and DMSO (right).

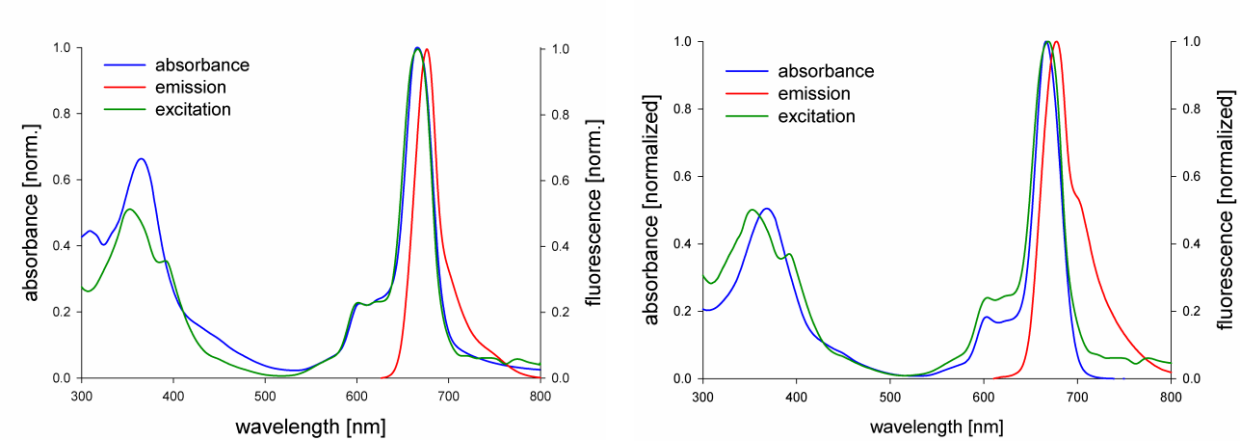

Fig. S41. Absorbance, emission and excitation spectra of **8** in DMF (left) and DMSO (right).

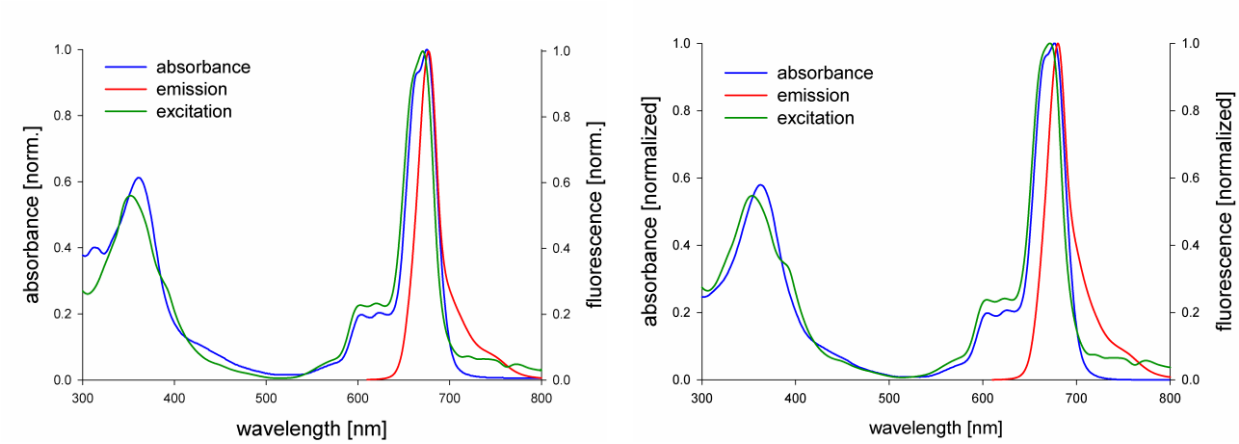

Fig. S42. Absorbance, emission and excitation spectra of **9** in DMF (left) and DMSO (right).

Synthetic approaches towards porphyrazines bearing 4-(benzyloxy)phenyl substituents

2,3-Dicyanopyrazine derivative **5b**, similarly to its **5a** and **5c** analogues, was used in macrocyclisation reactions leading to porphyrazines, following general procedures described in article. Symmetrical A_4-type porphyrazine **10** and tribenzoporphyrazine A_3B-type **11** were obtained (**Fig. S43**). Formation of desired chemicals was confirmed by the means of high-resolution mass spectrometry (MALDI-TOF HRMS) – **Fig S44** and **S47**. Low solubility of porphyrazine **10** unabled its purification by means of column chromatography. Crude product has been precipitated from reaction mixture, filtered and rinsed with: CH_2Cl_2, THF, ethyl acetate and acetone. Obtained green powder was subsequently subjected to NMR analysis, using DMSO-d_6 as a solvent. Slightly better solubility was observed for porphyrazine **11**. Crude product was chromatographed on silica gel using DCM, hexanes/ethyl acetate (7:2) and CH_2Cl_2/MeOH (200:1). Subsequenlty , obtained product was analyzed by means of NMR, using pyridine-d_5 as a solvent. In both cases, strong tendency to form aggregated species resulted in poorly resolved NMR spectra and therefore, uncertain results of the NMR analysis (**Fig. S45**, **S46**, **S48**, **S49**).

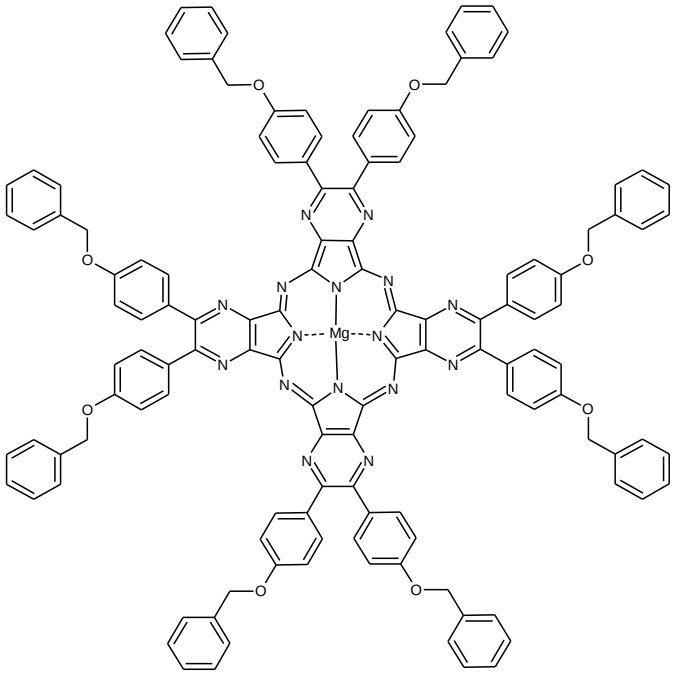

10

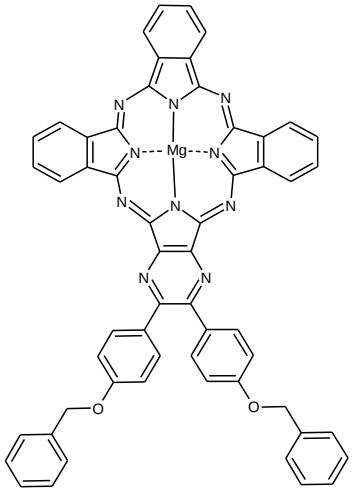

11

Fig. S43. Structures of porphyrazines **10** and **11** bearing 4-(benzyloxy)phenyl substituents.

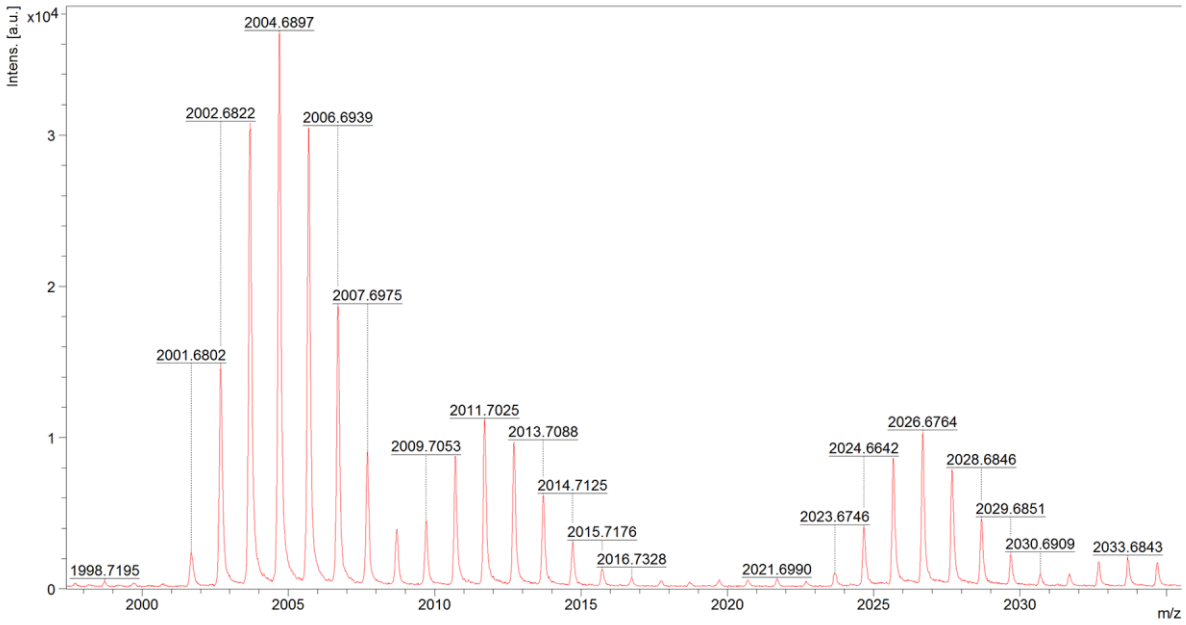

Fig. S44. MALDI-TOF HRMS spectrum of **10.** Calculated mass for $C_{128}H_{88}MgN_{16}O_8$ $[M]^+$ 2001,6851, found: *m/z* 2001,6802; for $C_{128}H_{88}MgN_{16}NaO_8$ $[M+Na]^+$ 2024,6749, found: *m/z* 2024,6642.

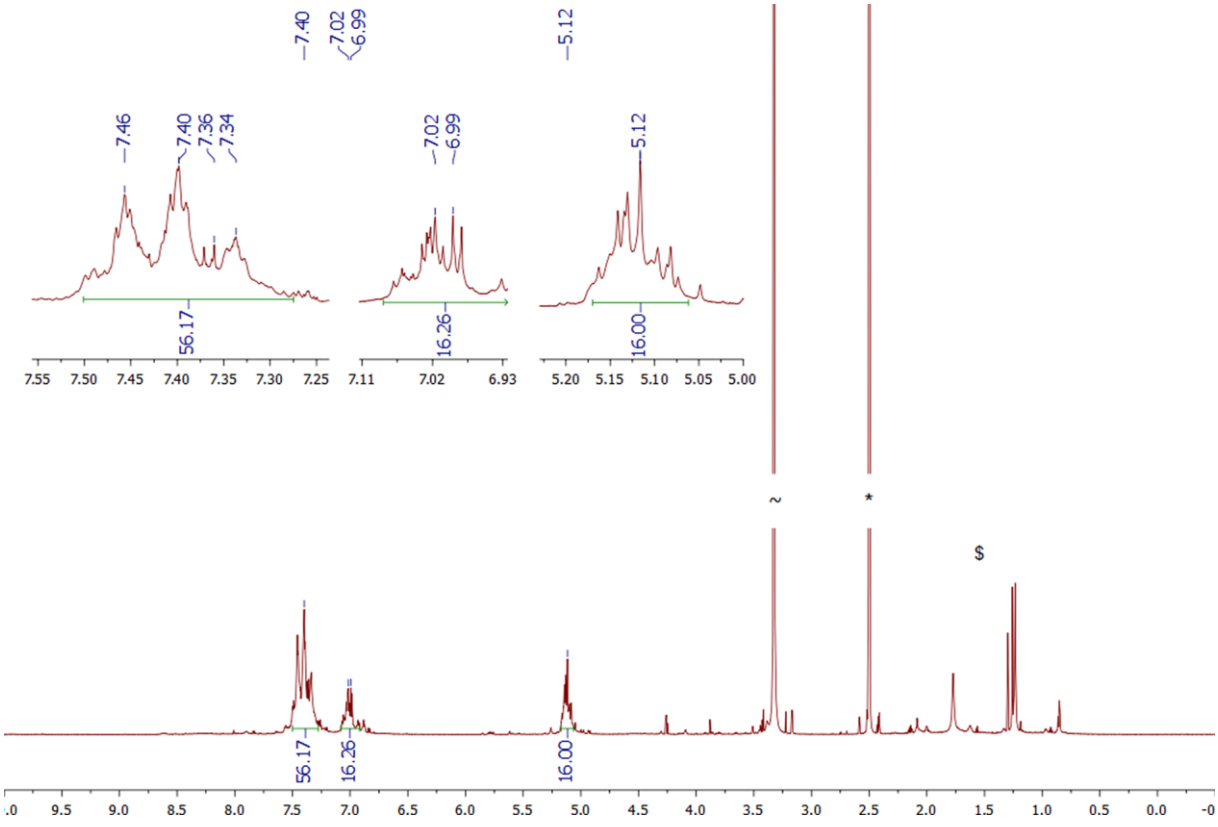

Fig. S45. ^{1}H NMR spectrum of **10** (800 MHz, DMSO-d_6, 298 K). The symbols *, ~ and $ indicate DMSO-d_6, water and hexane residual peaks, respectively.

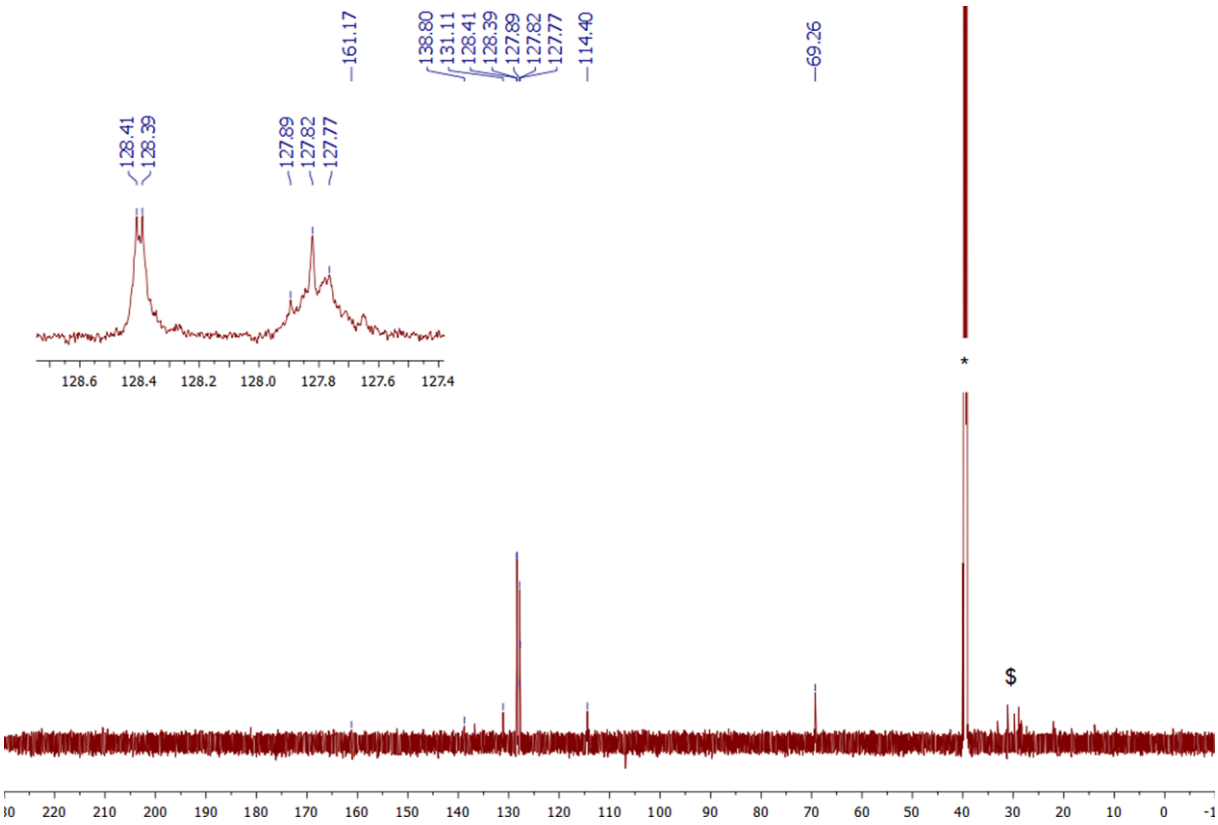

Fig. S46. ^{13}C NMR spectrum recorded for **10** (201 MHz, DMSO-d_6, 298 K). The symbols * and $ indicate DMSO-d_6 and hexane residual peaks, respectively.

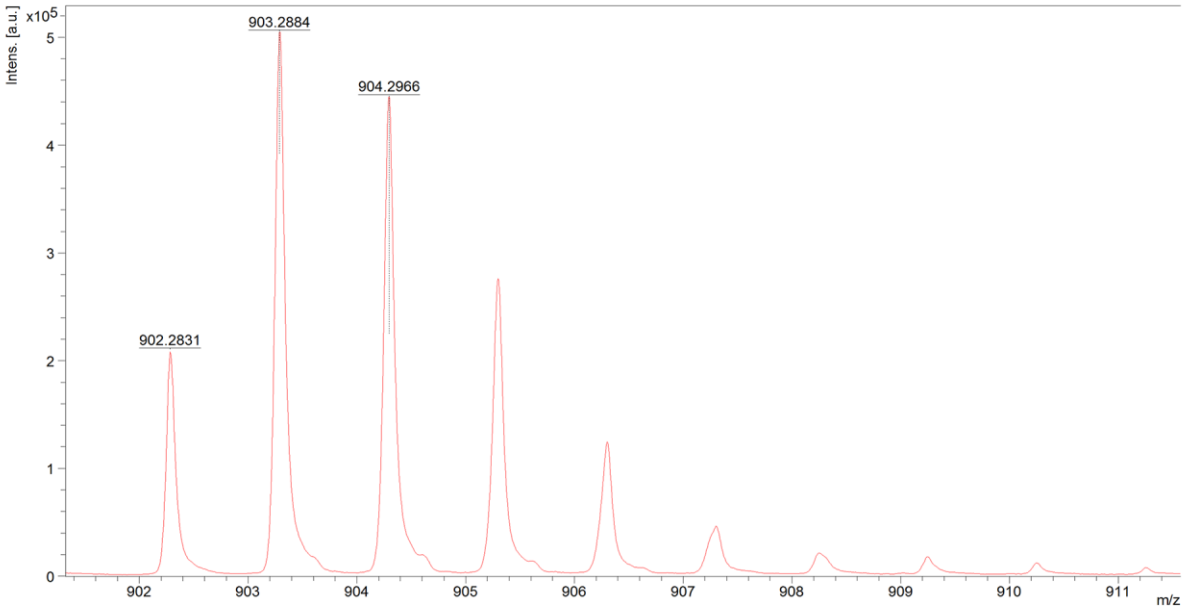

Fig. S47. MALDI-TOF HRMS spectrum of **11.** Calculated mass for $C_{56}H_{35}MgN_{10}O_2$ $[M+H]^+$ 903.2795, found: m/z 903.2884.

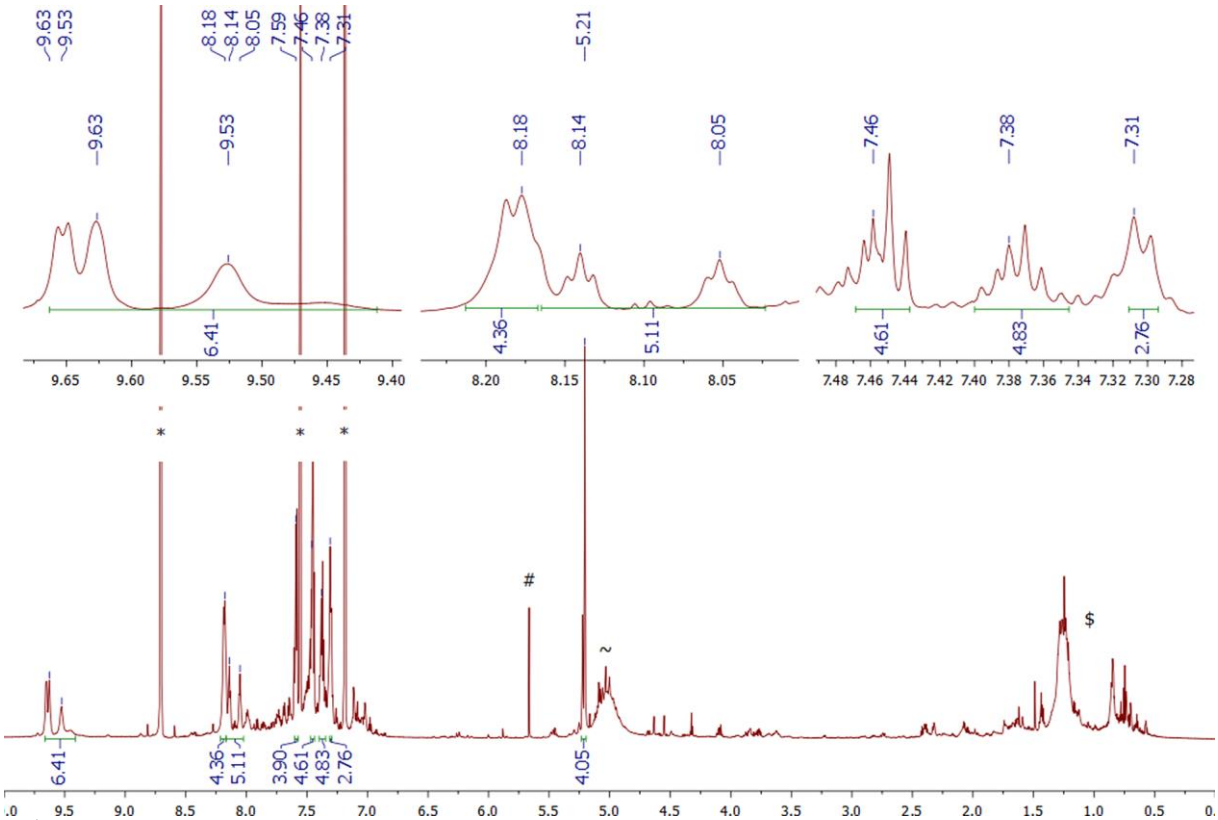

Fig. S48. ^{1}H NMR spectrum of **11** (800 MHz, pyridine-d_5, 298 K). The symbols *, #, ~ and $ indicate pyridine-d_5, CH_2Cl_2, water and hexane residual peaks, respectively.

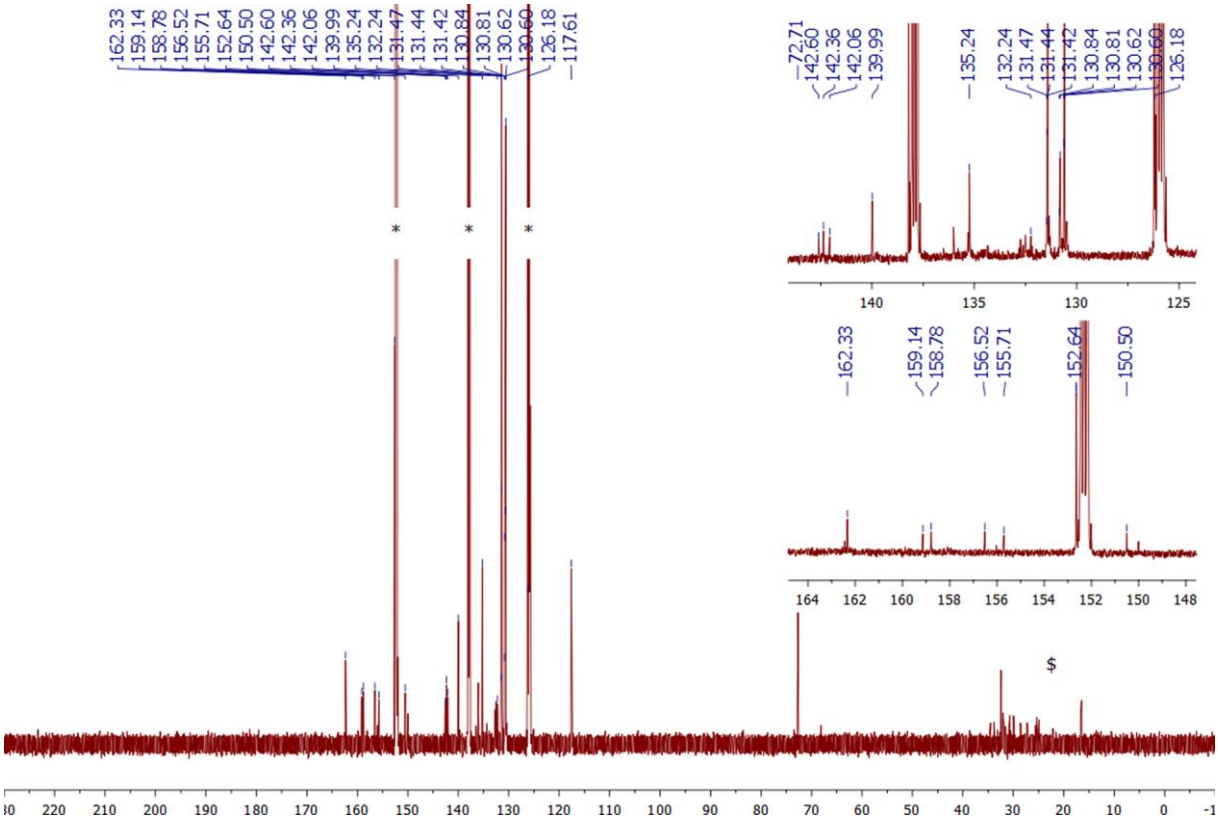

Fig. S49. ^{13}C NMR spectrum recorded for **11** (201 MHz, pyridine-d_5, 298 K). The symbols * and $ indicate pyridine-d_5 and hexane residual peaks, respectively.